Title
Fuzzy Logic Traction Controllers And Their Effect On Longitudinal Vehicle Platoon Systems

Authors
Bauer, M.
Tomizuka, M.

Publication Date
1995

CALIFORNIA PATH PROGRAM
INSTITUTE OF TRANSPORTATION STUDIES
UNIVERSITY OF CALIFORNIA, BERKELEY

Fuzzy Logic Traction Controllers and Their Effect on Longitudinal Vehicle Platoon Systems

M. Bauer
Masayoshi Tomizuka

California PATH Research Report
UCB-ITS-PRR-95-14

This work was performed as part of the California PATH Program of the University of California, in cooperation with the State of California Business, Transportation, and Housing Agency, Department of Transportation; and the United States Department of Transportation, Federal Highway Administration.

Report for MOU 035

May 1995

ISSN 1055-1425

Fuzzy Logic Traction Controllers and their Effect on Longitudinal Vehicle Platoon Systems

M. Bauer and Masayoshi Tomizuka

Department of Mechanical Engineering
University of California, Berkeley

Abstract:
The objective of this paper is to present fuzzy logic traction controllers and their effect on longitudinal vehicle platoon systems. A fuzzy logic approach is appealing for traction control because of the non-linearities and time-varying uncertainties in traction control systems. Two fuzzy logic traction controllers are presented. One fuzzy controller estimates the "peak slip" corresponding to the maximum tire-road adhesion coefficient and regulates wheel slip at that value. The other fuzzy logic controller regulates wheel slip at any desired value. The controllers' performance and robustness against changing road conditions and time-varying uncertainty is evaluated by simulation. The effect of traction control on longitudinal vehicle platoon systems is studies by simulation also. The simulations included acceleration and deceleration maneuvers on an icy road. The results indicate that traction control may substantially improve longitudinal platoon performance, especially when icy road conditions exist.

Executive Summary:

This paper presents two fuzzy logic traction controllers and investigates their effect on longitudinal platoon systems. A fuzzy logic approach is appealing for traction control because of the non-linearities and time-varying uncertainties involved in traction control systems.

Traction controllers regulate wheel slip, the normalized difference between wheel and vehicle speed. Wheel slip strongly influences the tire-road adhesion coefficient. The fastest stable acceleration and deceleration is achieved by maximizing the adhesion coefficient (Kachroo 1994). This means regulating slip at the "peak slip", which corresponds to the maximum of the $\mu - \lambda$ curve. Stable vehicle motion is achieved by maintaining the magnitude of wheel slip at or below the "peak slip".

The fuzzy logic traction controllers presented in this paper regulate brake torque to control wheel slip. One fuzzy controller estimates the "peak slip" corresponding to the maximum tire-road adhesion coefficient and regulates wheel slip at that value. The controller is attractive because of its ability to maximize acceleration and deceleration regardless of road condition. However, we found through simulations that the controller's performance degrades in the presence of time-varying uncertainties. The other fuzzy logic controller regulates slip at any desired value. Through simulations we found the controller to be robust against changing road conditions and uncertainties. The target slip is predetermined, and not necessarily the peak slip for all road conditions. However if the target slip is set low, stable acceleration and deceleration is guaranteed, regardless of road condition.

Traction controllers can improve longitudinal platooning ability by regulating wheel slip to provide the necessary tractive forces during longitudinal maneuvers. Using simulations we evaluated the effect of traction control on longitudinal platoon systems. The simulations included acceleration and deceleration maneuvers on an icy road. The results indicate traction control substantially improves longitudinal platoon performance with icy road conditions. Traction control also provides additional safety if emergency stopping or acceleration is required.

Future research, not within the scope of this report, should be performed to:

- Develop fuzzy controller that combines both brake torque and engine torque regulation.
- Enhance the fuzzy controller and longitudinal vehicle platooning simulations to include cornering maneuvers using a four-wheel (full car) model.
- Experimentally validate the fuzzy traction controllers presented in this paper.
- Experimentally demonstrate the advantages of traction control in longitudinal vehicle platoon systems.

1. Introduction

Traction controllers improve a driver's ability to control a vehicle under adverse conditions, such as a wet or icy road. They provide for fast and stable acceleration and deceleration by maximizing the tractive force between the vehicle's tires and the road (Tan 1988, Tan 1989, Leiber 1983, Layne 1993, Kachroo 1994). They also improve steerability by preventing the wheels from slipping (Tan 1988, Kachroo 1994). Since effective control of a vehicle's motion is essential for lateral and longitudinal guidance systems, traction control becomes an important part of highway automation.

Traction controllers regulate wheel slip, the normalized difference between wheel and vehicle speed. Wheel slip strongly influences the tire-road adhesion coefficient. Figure 1 shows a typical slip (λ) adhesion coefficient (μ) curve for various road conditions (Harned et al. 1983).

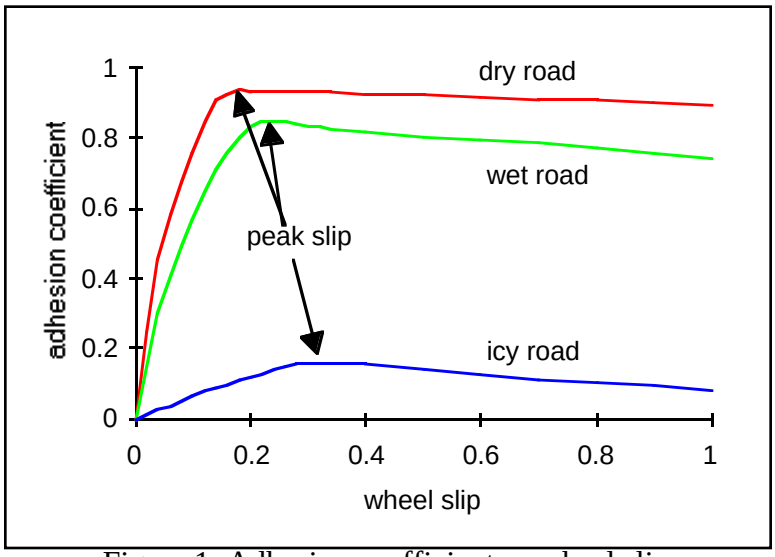

Figure 1: Adhesion coefficient vs wheel slip (acceleration)

The level at which the controllers should regulate wheel slip depends on the control objective to be met. The fastest stable acceleration and deceleration is achieved by maximizing the adhesion coefficient (Kachroo 1994). This means regulating slip at the "peak slip", which corresponds to the maximum of the $\mu - \lambda$ curve. Operating in the negative slope region of the $\mu - \lambda$ curve reduces system stability and cornering ability, and increases sensitivity to disturbances (Tan 1988). Stable vehicle motion is achieved by maintaining the magnitude of wheel slip at or below the "peak slip".

Control of wheel slip is important in highway automation systems. Traction controllers can improve both lateral path following and longitudinal platooning performance. Traction controllers regulate wheel slip to improve steerability during lateral maneuvers (Tan 1988). Traction controllers can also improve longitudinal platooning ability by regulating wheel slip to provide the necessary tractive forces during longitudinal maneuvers. In addition, traction control improves emergency acceleration and braking ability.

The design of a traction control system is complicated by several factors. The system is highly non-linear, vehicle parameters and road conditions may change significantly with time,

and the tire-road interaction is difficult to measure and estimate (Tan 1988, Tan 1989, Leiber 1983, Layne 1993, Kachroo 1994).

Traction controllers based on conventional control approaches have been successfully designed and implemented. Gain scheduling traction controllers (Lieber 1983, Schurr 1984) and robust control algorithms based on sliding mode theory have been developed (Tan 1988, Tan 1989, Kachroo 1994). The uncertainty and non-linearity associated with traction control makes a fuzzy-logic control approach appealing (Layne 1993, Tong 1977, Lee 1990, Wang 1992).

In this paper, we first describe a dynamic model for traction control. Then we present two fuzzy-logic traction controller designs and evaluate them using simulations. Lastly, we present the results of simulations used to evaluate the effect of traction control on longitudinal platoon systems.

2. DYNAMIC MODEL FOR TRACTION CONTROL

The system dynamics used for simulation include a simple linear car model, a one wheel rotational model, an engine model and actuator models. Only longitudinal dynamics are considered. The simulation dynamics are based on the following assumptions:

- The vehicle is front wheel drive with a rigid drive axle
- The brake force is divided evenly between the front wheels
- The brakes obey first order dynamics
- The ideal gas law holds in the intake manifold and the temperature of the intake manifold is constant
- The road is flat
- The road surface condition is the same for all tires.

2.1 Wheel Model

Figure 2 shows a model for one wheel rotational dynamics. The wheel rotational equation is (Tan 1988)

$$\frac{d\omega}{dt} = \frac{1}{J}\cdot[T_e - T_b] - \frac{R_w}{J}\cdot F_t - \frac{R_w}{J}\cdot F_w \qquad (1)$$

where

ω = wheel rotational speed
T_b = brake torque
T_e = engine torque
F_t = traction force
F_w = viscous friction force ($F_w = B\cdot\omega$)
J = wheel inertia
R_w = wheel radius
B = viscous friction coefficient

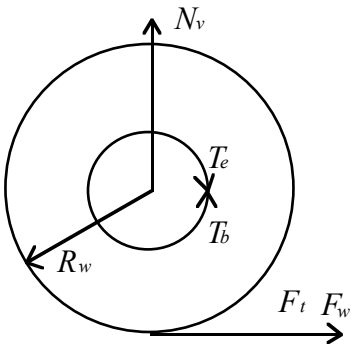

Figure 2: Wheel Model
(acceleration)

The tractive force is

$$F_t = N_v \cdot \mu \qquad (2)$$

where

$\mu = f(\lambda)$ (ref. fig. 1)
$\lambda = [\omega_w - (V / R_w)] / \omega_w$ (acceleration)
$\lambda = [\omega_w - (V / R_w)] / (V / R_w)$ (deceleration)
N_v = normal load on tire μ = adhesion coefficient
V = vehicle speed λ = wheel slip

2.2 Car Model

The dynamic equation for a vehicle model (fig. 3) is (Tan 1988)

$$\frac{dV}{dt} = \frac{N_w}{M_v} \cdot F_t - \frac{1}{M_v} \cdot F_d \qquad (3)$$

where

F_d = wind drag force $(F_d = C \cdot V^2)$ N_w = number of driving wheels (acceleration)
M_v = car mass N_w = number of braking wheels (deceleration)

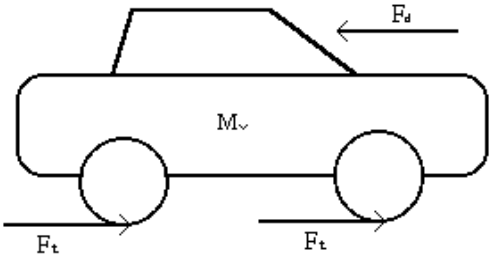

Figure 3: Car Model
(acceleration)

C = wind drag coefficient

2.3 Engine Model

The engine model consists of intake manifold and engine speed dynamics (Tomizuka 1993). The intake manifold equation is

$$\frac{dm_{ai}(\omega_e, P_m)}{dt} = \beta \cdot f_1(P_m/P_a) \cdot TC(\alpha) \qquad (4)$$

where

m_{ai} = air mass flow rate
ω_e = engine speed
P_m = intake manifold air pressure
β = maximum possible airflow rate constant
P_a = atmospheric function
f_1 = pressure ratio influence function
α = throttle valve angle
TC = throttle valve characteristic

The engine speed equation is

$$\frac{d\omega_e}{dt} = \frac{1}{J_e} \cdot T_e(\omega_e, P_m) \qquad (5)$$

where

J_e = effective engine inertia

Typically the air mass flow rate and engine torque are provided by the engine manufacturer as a look up table.

2.4 Actuator Models

Brake and throttle angle actuators are required for traction control and longitudinal platoon control. We use first order brake and throttle angle actuator dynamics in our model (Swaroop 1994).

The brake actuator equation is

$$\frac{dT_b}{dt} = \frac{T_{bc} - T_b}{\tau_b} \qquad (6)$$

where

T_{bc} = command (desired) brake torque
τ_b = brake time constant

The throttle actuator is

$$\frac{d\alpha}{dt} = \frac{\alpha_c - \alpha}{\tau_\alpha} \qquad (7)$$

where

α_c = command (desired) throttle angle
τ_α = throttle angle time constant

3. FUZZY LOGIC TRACTION CONTROLLERS

Fuzzy logic controllers provide a means of converting a linguistic control strategy, usually based on expert knowledge, into an automatic control strategy. Fuzzy set theory (Zadeh 1965), on which fuzzy controllers are based, allows imprecise and qualitative information to be expressed in a quantitative way to be processed for decision making (Tong 1977). Because fuzzy logic controllers deal with inexactness in a rigorous manner, they are effective at handling the uncertainties and non-linearities associated with complex systems like traction control. Some fuzzy logic controller basics are given in appendix 1.

We will present two fuzzy logic traction controllers. The first estimates the peak of the $\mu - \lambda$ curve and regulates the slip at the peak. The second maintains the slip at any desired value. We evaluated the controllers' performance using simulation. The dynamics of a wheel's acceleration and deceleration are essentially the same. We concentrate mainly on the acceleration case. The controllers (we designed) for acceleration (anti-slip) control can easily be enhanced to include deceleration (anti-lock) control, which will be presented in section 4 where we investigate the effect of traction control on longitudinal control.

Anti-slip controllers modulate the torque acting on the driving wheels only, either by controlling engine torque, brake torque or both. Engine torque is controlled by adjusting the throttle angle and/or by interrupting the fuel injection. Brake torque is controlled by modulating the brake pressure with a brake pressure booster and solenoid valves.

The advantage of a system that controls only engine torque is that since brakes are not used, no brake wear occurs. The disadvantage is that since engine torque is distributed evenly between driving wheels by the differential, the torque at each driving wheel cannot be controlled individually and, as a result, traction is not maximized on μ-split road surfaces. The torque at both driving wheels is set to prevent the wheel with the lower adhesion coefficient from slipping and the full traction capacity of the wheel with the higher adhesion coefficient is not taken advantage of.

With brake torque modulation, the torque at each driving wheel is controlled individually and traction is maximized, even on μ-split road surfaces. The system is relatively inexpensive because the necessary hardware is essentially the same as that used for anti-lock brake control. The disadvantage of a "brake only" system is that the brakes may be subjected to high loads for long periods of time, which may cause excessive brake wear.

Some anti-slip controllers combine both engine torque and brake torque control. On homogenous road surfaces, only engine torque control is used to prevent slip. On μ-split road surfaces, both engine and brake torque control are used. The engine torque is reduced to prevent the wheel with the higher adhesion coefficient from slipping and the torque at the wheel with the lower adhesion coefficient is further reduced with brake action to prevent it from slipping. The disadvantage of the system is its complexity and cost.

We designed fuzzy logic anti-slip controllers that modulate brake torque only. It may be worthwhile in the future to investigate fuzzy logic traction control schemes that modulate engine torque as well as brake torque. Especially since the vehicles used in highway automation systems will already be equipped with a throttle angle actuator. The fuzzy control algorithms used to regulate brake torque could most likely also be used to regulate engine torque with only minimal modification.

Anti-skid controllers regulate wheel slip by modulating brake torque, usually at all four wheels. Several different implementation schemes are used. The most popular features

individual brake torque control for the front wheels and "select low" brake torque control for the rear wheels (Kraft 1990, Rittmannsberger 1988, Sigi 1990, Kiyotaka 1990). Individual control of the front wheels' brake torque allows the traction force at both wheels to be maximized, even on μ-split road surfaces. Although the front wheels may have different applied brake torques, with minimal steering, vehicle stability can be maintained. The select low principle used for the rear wheels means the brake torque at both wheels is identical and set to prevent the wheel with the lower adhesion coefficient from slipping. Since both wheels are braked evenly, rear wheel traction will not be maximized on μ-split road surfaces, but stability will be maintained. Uneven rear wheel braking can cause the vehicle's rear end to slide, which is difficult to control. Because front braking is more stable than rear braking, the system is designed to concentrate the braking force on the front tires. Typically, 70% to 80% of the total brake force is applied to the front wheels (Kraft 1990, Rittmannsberger 1988).

In our simulations, we implement the fuzzy logic traction controllers to act on the front brakes only. Assuming the vehicle is front wheel drive, actual anti-slip controllers would also only act on the front brakes. Considering most of the traction force during braking in actual systems comes from the front wheels, anti-lock control with braking on the front wheels only is a good approximation.

3.1 Traction Control with Peak Slip Estimation

Our control objective is to regulate wheel slip at the peak slip during acceleration and in the positive slope region of the $\mu - \lambda$ curve otherwise. We designed a traction controller that estimates the peak slip and maintains wheel slip at the peak slip. Although peak slip changes with road condition, the controller should provide for the fastest stable acceleration for all road conditions.

3.1.1 Controller Design

The traction controller is essentially the same as a fuzzy logic controller designed to prevent slip in an electric motor coach (Schurr 1984). The $\mu - \lambda$ curve was used as a model to develop the fuzzy control rules (fig. 4).

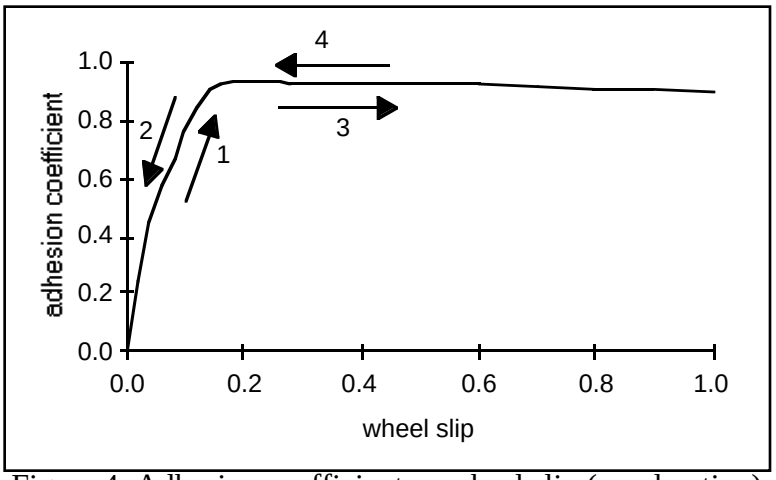

Figure 4: Adhesion coefficient vs wheel slip (acceleration)

The fuzzy rule set is based on the following logic (the numbers below correspond to the numbers in fig. 4):

1 - If $d\lambda/dt$ is positive and $d\mu/dt$ is positive, decrease brake torque a little.
2 - If $d\lambda/dt$ is negative and $d\mu/dt$ is negative, decrease brake torque a lot.
3 - If $d\lambda/dt$ is positive and $d\mu/dt$ is negative, increase brake torque a lot.
4 - If $d\lambda/dt$ is negative and $d\mu/dt$ is positive, increase brake torque a little.

Time derivatives of the adhesion coefficient and the wheel slip are not directly measurable, and they are approximated as follows.

Controller Inputs:

$d\lambda/dt$ is estimated as the change in λ over one sample period:

$$\frac{\Delta\lambda}{\Delta t} = \frac{\lambda_N - \lambda_{N-1}}{t_N - t_{N-1}} \qquad (8)$$

$d\mu/dt$ is estimated from the change in vehicle acceleration over one sample period. To justify this, we first note from eqns. (2) and (3)

$$\mu(t) = \frac{M_v \cdot N_V}{N_w} \cdot \dot{V}(t) + M_v \cdot N_V \cdot F_d(t)$$

Therefore, the change in the adhesion coefficient over one sample period is

$$\Delta\mu \approx \frac{M_v \cdot N_V}{N_w} \cdot (\dot{V}_N - \dot{V}_{N-1}) + M_v \cdot N_V \cdot (F_{dN} - F_{dN-1})$$

Assuming the change in acceleration is much larger than the change in drag force over one sample period (i.e.$(\dot{V}_N - \dot{V}_{N-1}) >> (F_{dN} - F_{dN-1})$),

$$\frac{\Delta\mu}{\Delta t} \approx \frac{K(\dot{V}_N - \dot{V}_{N-1})}{t_N - t_{N-1}} \qquad (9)$$

The estimate of $\Delta\lambda$ requires measurements of the vehicle and wheel speeds ($\lambda = [\omega_w - (V / R_w)] / \omega_w$). Notice that λ must be calculated based on the vehicle speed and the wheel speed. In a proposed PATH scenario for highway automation utilizing magnetic markers for lateral guidance, the vehicle speed can be obtained by measuring the travel time of the vehicle from one marker to the next (Tomizuka 1993). The wheel speed is normally available from a tachometer or an encoder. The estimate of $\Delta\mu$ requires measurement of the vehicle acceleration. Vehicle acceleration may be available from the vehicle speed measurement using magnetic markers as outlined above, or can be obtained from an accelerometer.

Controller output:

The controller output is change in desired brake torque (ΔT_{bc}). The desired brake torque (T_{bc}) becomes

$$T_{bc} = T_{bc} + \Delta T_{bc}$$

Membership Functions:

As reviewed in appendix 1, membership functions for fuzzy sets such as zero and positive small in fuzzy rules must be defined. In this work, both controller inputs and the controller output have the same triangular membership function (fig. 5). It has five grades; positive big (pb), positive small (ps), zero (zo), negative small (ns) and negative big (nb).

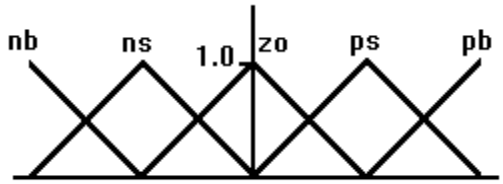

Figure 5: Five grade triangular membership function

Fuzzy Rule Table:

The fuzzy rules are of the form:

If $d\lambda/dt$ is positive big and $d\mu/dt$ is positive small, then ΔT_{bc} is negative small.

We used Larson's product operation rule as a fuzzy implication function and the center of area method for defuzzification (Lee 1990). An explanation of both is given in appendix 1. Figure 6 shows the fuzzy rule table.

		$d\lambda/dt$				
		pb	ps	zo	ns	nb
$d\mu/dt$	pb	ns	ns	zo	ps	ps
	ps	ns	ns	zo	ps	ps
	zo	pb	ps	zo	ns	ns
	ns	pb	ps	zo	ns	nb
	nb	pb	pb	zo	nb	nb

Figure 6: Fuzzy rule table with peak slip estimation (acceleration)

The fuzzy rule table could also be used to provide anti-lock control during braking by using the absolute value of slip and changing the sign of the output, change in desired brake torque.

3.1.2 Simulation Results:

We evaluated the performance of the traction controller for the acceleration case by simulation. The simulation model includes engine, vehicle, wheel and actuator dynamics (described in section 2). The simulations were performed with the vehicle having an initial throttle angle of 5 degrees, an initial speed of 5 m/s and essentially zero slip. To produce a slip condition, the desired throttle angle was stepped from 5 degrees to 85 degrees, which is approximately the saturated throttle angle. This simulates a driver "flooring" the accelerator

pedal. The vehicle parameters were modeled after a Lincoln Towncar, and are summarized in appendix 2. The tire-road model we used is described in section 2.

The purpose of the simulations is to study the initial low velocity transient response occurring as the throttle angle is stepped to 85 degrees. The initial low velocity transient represents slip occurring as the driver "floors" the accelerator pedel. The graphs displaying the simulation results show the initial transient response following the step input in desired throttle angle, which occurs at time zero. We evaluated the controller with the following three scenarios:

- Dry, wet and icy road conditions
- Constant uncertainty ($\pm$ 25%)
- Time varying uncertainty ($\pm$ 25%) .

Dry, Wet and Icy Road Conditions:

The controller was designed to regulate slip at the peak slip regardless of road condition. The $\mu - \lambda$ curve for each road condition has a different shape and peak slip value, so we tested the controller for three (dry, wet and icy). Figures 7-9 show the initial transient response of the front wheel slip and brake torque with and without traction control for each road condition.

From figure 1, the peak slips for dry, wet and roads are approximately 0.20, 0.25 and 0.35, respectively. The simulation results indicate that the traction controller is able to accurately estimate peak slip for all three road conditions and limit the vehicle's slip at that value. Thus, the controller appears robust against changing road conditions.

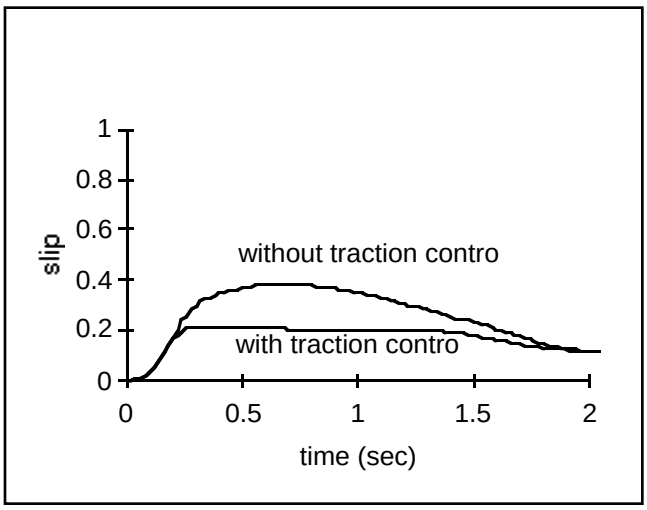

Figure 7(a): Slip vs time

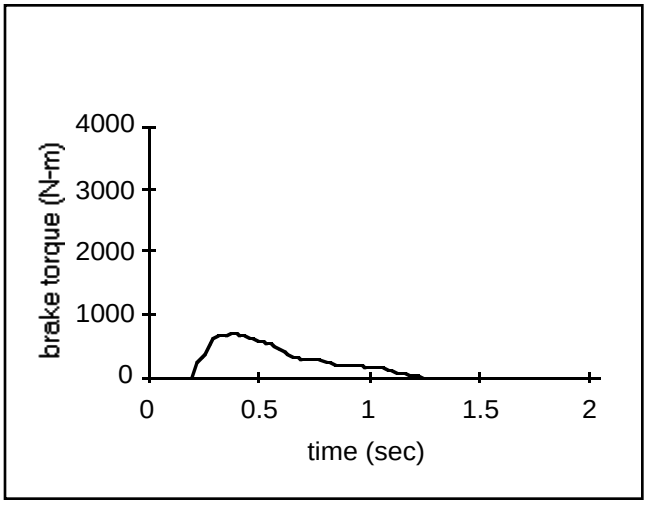

Figure 7(b): Brake torque vs time

Figure 7: Dry road (acceleration)

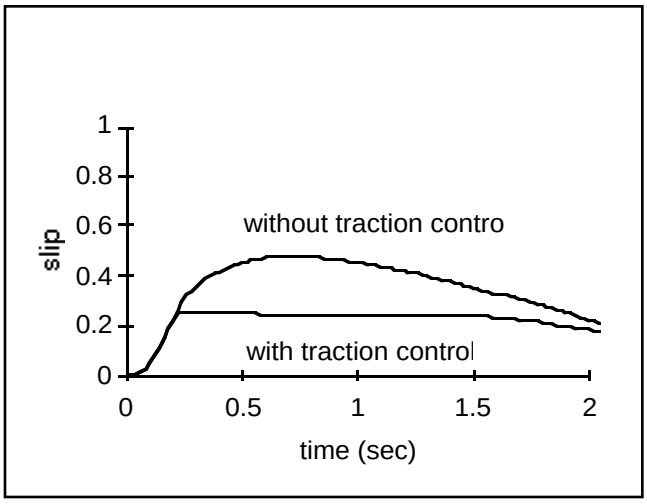

Figure 8(a): Slip vs time

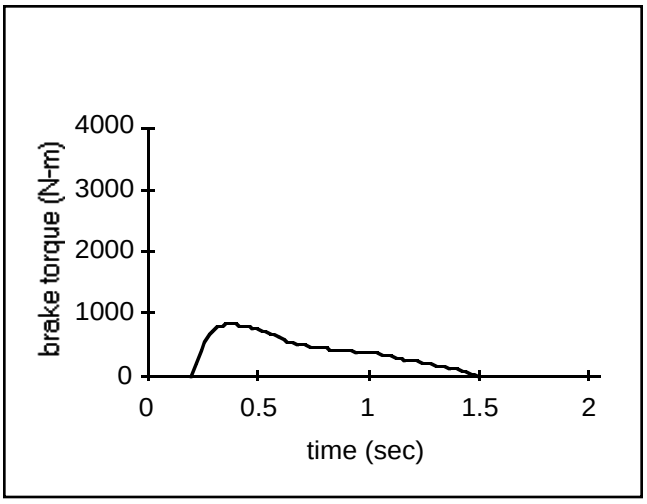

Figure 8(b): Brake torque vs time

Figure 8: Wet road (acceleration)

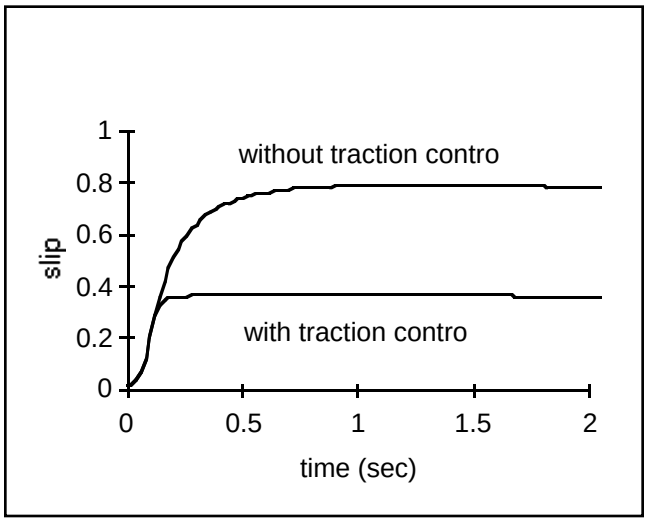

Figure 9(a): Slip vs time

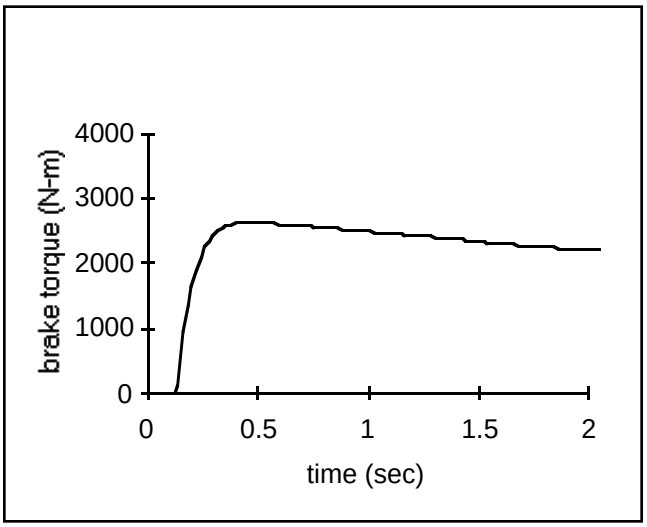

Figure 9(b): Brake torque vs time

Figure 9: Icy road (acceleration)

Constant Uncertainty:

As mentioned previously, traction controllers should be robust against uncertainties. We performed simulations to evaluate the fuzzy logic controller's ability to handle these uncertainties. First, we looked at constant uncertainty which was modeled as a ± 25% change in system lumped parameters. For example, eqn. (1) becomes:

$$\frac{d\omega}{dt} = (1+\Delta_1)\cdot\frac{1}{J}\cdot[T_e - T_b] - (1+\Delta_1)\cdot\frac{R_w}{J}\cdot F_t - (1+\Delta_1)\frac{R_w}{J}\cdot F_w \qquad |\Delta_1| \le 0.25$$

Equation (3) is modified in the same manner.

Figure 10 shows the results of simulations with no uncertainty, +25% constant uncertainty and −25% constant uncertainty. Figure 10(a) shows identical wheel slip results for all cases, indicating the controller is robust against constant uncertainty. The effect of the uncertainty shows up in the controller's output, brake torque (fig. 10(b)).

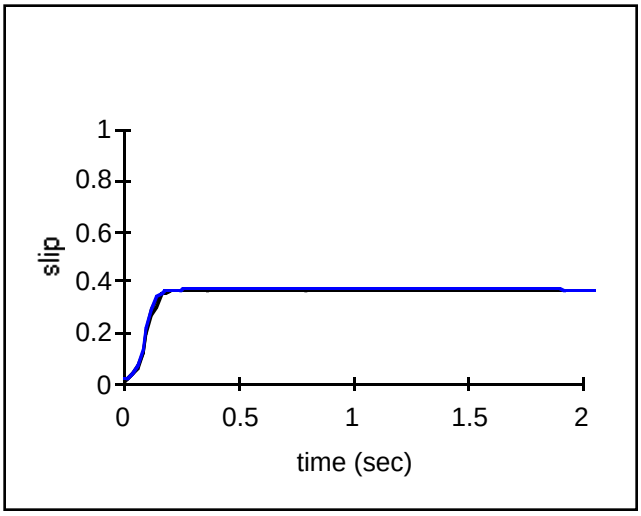

Figure 10(a): Slip vs time

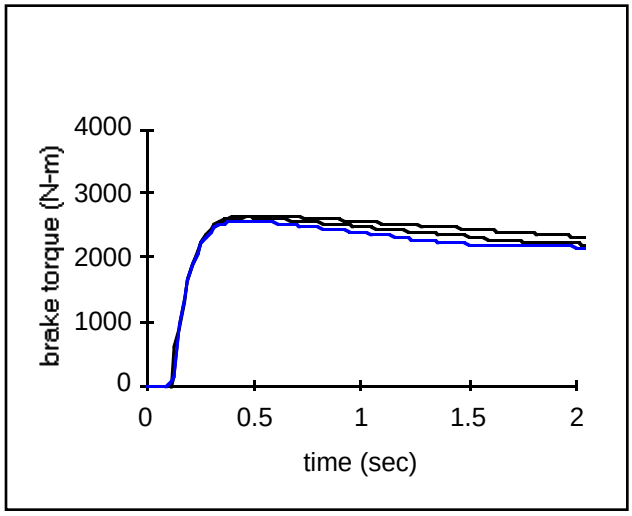

Figure 10(b): Brake torque vs time

Figure 10: Wet road, no uncertainty, +25% constant uncertainty and −25% constant uncertainty (acceleration)

Time Varying Uncertainty:

Vehicle parameters change with time. For example, an engine or tire imbalance may cause vehicle parameter oscillations. We modeled this condition as ±25% sinusoidal uncertainty ($\Delta_1 = 1 + 0.25\cdot\sin(\omega\cdot t)$).

Figure 11 shows results with ±25% sinusoidal uncertainty of frequency 4π. The controller is unable to maintain slip at the "peak slip". With time-varying uncertainty, it is difficult to accurately estimate the controller input $d\mu/dt$, which is used to determine the system's operating point on the $\mu - \lambda$ curve. The change in adhesion coefficient is estimated from the change in vehicle acceleration (eqn. 9), which is effected by the time-varying uncertainty. To illustrate this point, we ran simulations with the controller using the actual $d\mu/dt$ from fig. 1 as an input instead of the estimated $d\mu/dt$. The results are shown in fig. 12. The controller is able to maintain the slip at the "peak slip" and performs significantly better when the actual $d\mu/dt$ is used.

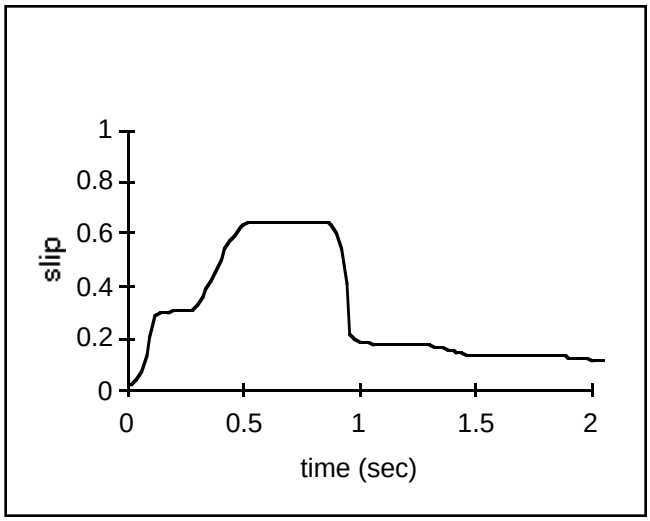

Figure 11(a): Slip vs time

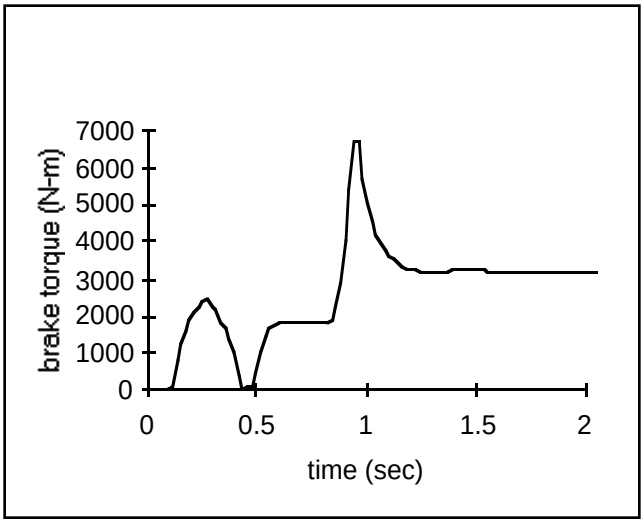

Figure 11(b): Brake torque vs time

Figure 11: Wet road, ±25% sinusoidal uncertainty, 4π frequency, estimated $d\mu/dt$ used as controller input (acceleration)

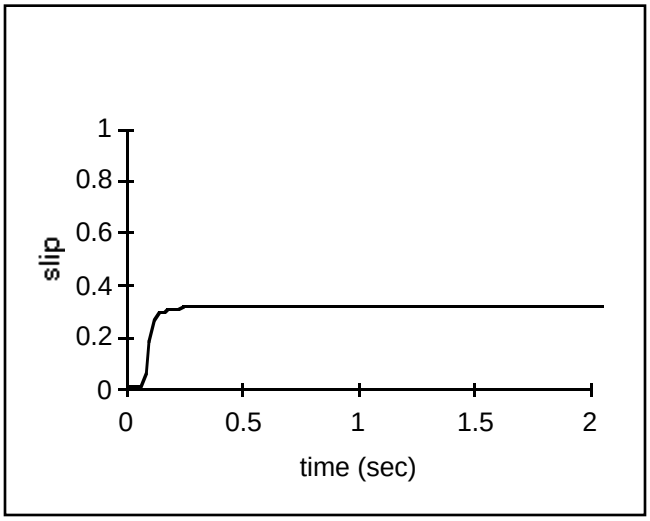

Figure 12(a): Slip vs time

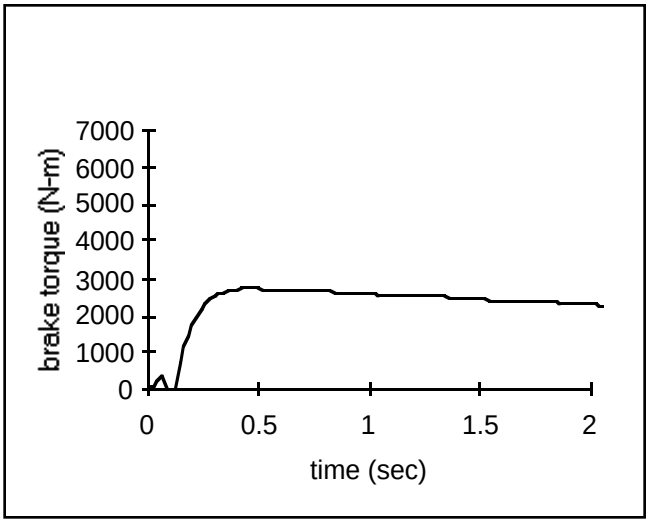

Figure 12(b): Brake torque vs time

Figure 12: Wet road, ±25% sinusoidal uncertainty, 4π frequency, actual $d\mu/dt$ used as controller input (acceleration)

The fuzzy controller is attractive because of its ability to estimate peak slip and maintain slip at that value regardless of road condition. We found the controller robust against constant parameter uncertainty. However, we found performance degrades when system parameters change quickly with time. The controller is limited because it requires an accurate estimate of $d\mu/dt$, which is difficult to get, especially with time-varying uncertainty.

Perhaps the robustness of the controller to time-varying uncertainty could be improved if the adhesion coefficient was directly measured instead of estimated from vehicle acceleration. A scheme to measure the adhesion coefficient using strain gauges mounted on the suspension has

been designed and tested by (Miyasaki 1990). The adhesion coefficient detector has strain gauges mounted on the front suspension strat and the rear axle housing to detect the shear strains proportional to the vertical load and traction force acting of the wheels. The strain gauge signals are processed to produce a voltage which is proportional to the adhesion coefficient.

3.2 Fuzzy Controller with Target Slip Regulation

In this section, we present a fuzzy logic traction controller that maintains wheel slip at any desired value (target slip). The advantage of the controller is that it does not use $d\mu/dt$ as an input, which we found difficult to estimate. Many traction controllers are designed to limit slip below 0.15 - 0.20 , which is at or below the peak of the $\mu - \lambda$ curve for most road conditions (Harned 1969, Layne 1993). The goal of the controllers is to prevent the slip from entering the negative slope region of the $\mu - \lambda$ curve.

3.2.1 Controller Design

Controller Inputs:

The controller inputs are the error (λ_{error}) and the change in error ($\Delta\lambda_{error}$).

$$\lambda_{error} = \lambda - \lambda_{target}$$

$$\frac{d\lambda_{error}}{dt} \approx \frac{\Delta\lambda_{error}}{\Delta t} = [\lambda_{error_N} - \lambda_{error_{N-1}}] / [t_N - t_{N-1}]$$

Controller output:

The output from the controller is the change in desired brake torque. The desired brake torque becomes

$$T_{bc} = T_{bc} + \Delta T_{bc}$$

Membership Functions:

Both controller inputs and the controller output have a five grade membership function (fig. 5).

Fuzzy Rule Table:

The fuzzy rules are of the same form as the previous controller. We use Larson's product operation rule as a fuzzy implication function and the center of area method for defuzzification. The fuzzy rule table is shown in fig. 13. As with the previous fuzzy controller, the fuzzy rule table could also be used to provide anti-lock control during braking by using the absolute value of slip and changing the sign of the output, change in desired brake torque.

		error				
		pb	ps	zo	ns	nb
derror/dt	pb	pb	pb	pb	ps	zo
	ps	pb	pb	ps	ns	ns
	zo	pb	ps	zo	ns	nb
	ns	ps	ps	zo	nb	nb
	nb	ps	ps	ns	nb	nb

Figure 13: Fuzzy rule table with desired slip regulation (acceleration).

3.2.2 Simulations

We evaluate by simulations the controller's performance with the same three scenarios as the controller described in section 3.1; different road conditions, constant uncertainty and time varying uncertainty. We set the target slip to 0.20.

Dry, Wet and Icy Road Conditions:

Figures 14, 15 and 16 show the results with dry, wet and icy road conditions, respectively. The controller was able to maintain the slip at the desired value for all road conditions. The controller is robust against changing road conditions.

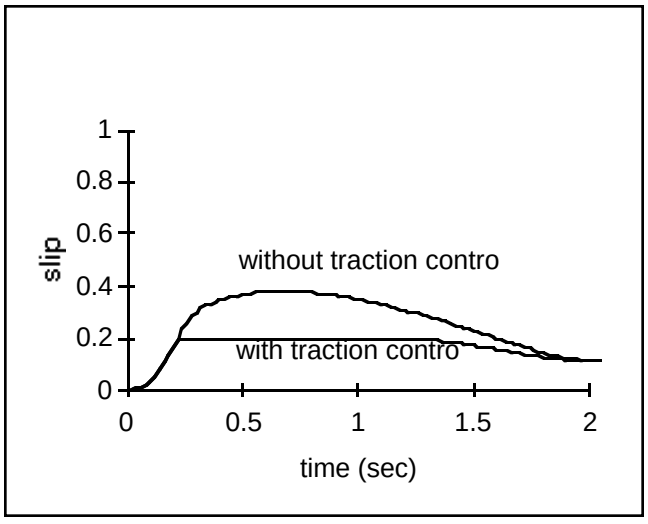

Figure 14(a): Slip vs time

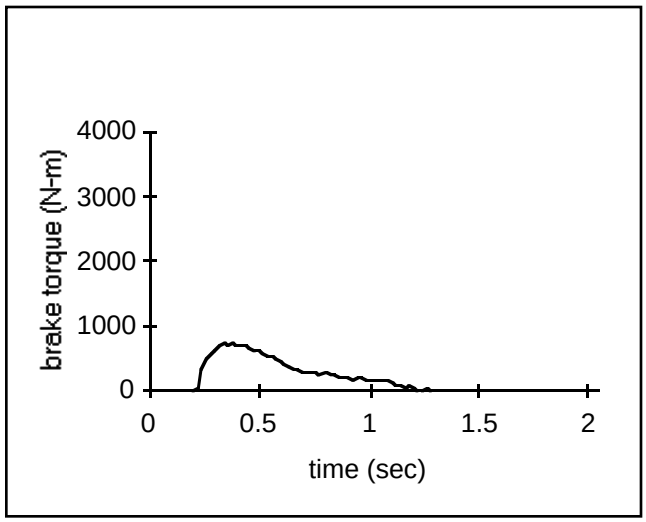

Figure 14(b): Brake torque vs time

Figure 14: Dry road, target slip = 0.20 (acceleration)

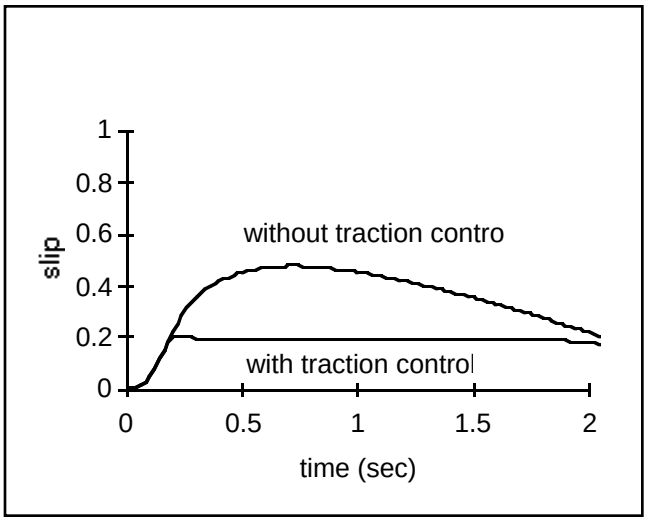

Figure 15(a): Slip vs time

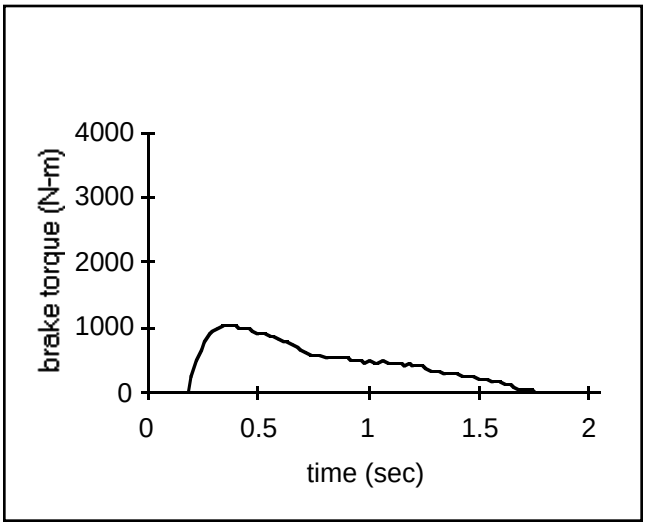

Figure 15(b): Brake torque vs time

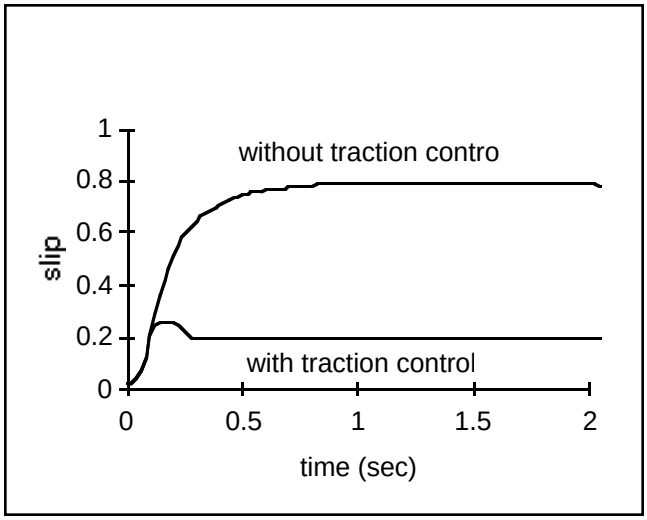

Figure 16(a): Slip vs time

Figure 15: Wet road, target slip = 0.20 (acceleration)

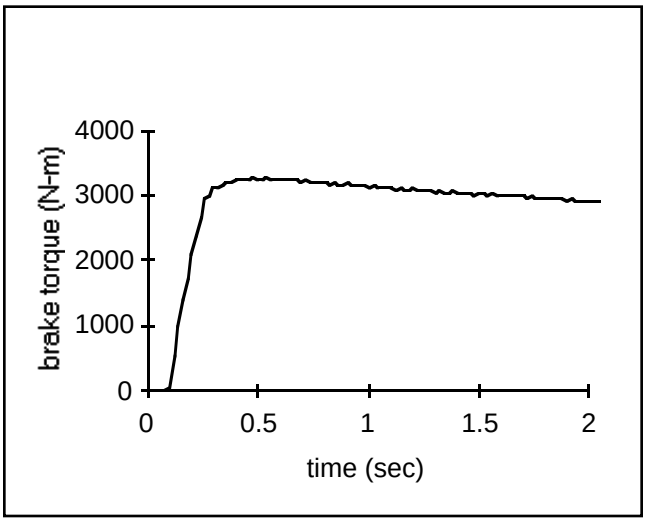

Figure 16(b): Brake torque vs time

Figure 16(a): Slip vs time

Constant Uncertainty:

Constant uncertainty was modeled the same as in the previous controller. We found the controller able to maintain slip at the target slip for all cases, no uncertainty, +25% constant uncertainty and −25% constant uncertainty.

Time Varying Uncertainty:

Figure 17 shows the results with ±25% sinusoidal uncertainty with 4π frequency. The controller was able to maintain slip at the target slip and appears robust against time-varying uncertainty.

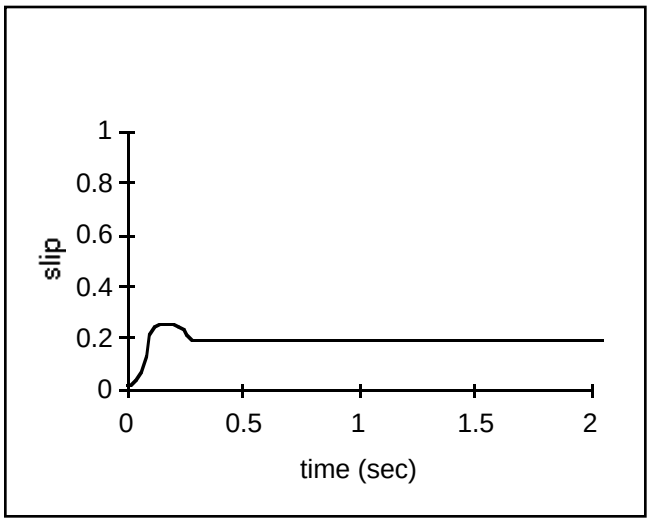

Figure 17(a): Slip vs time

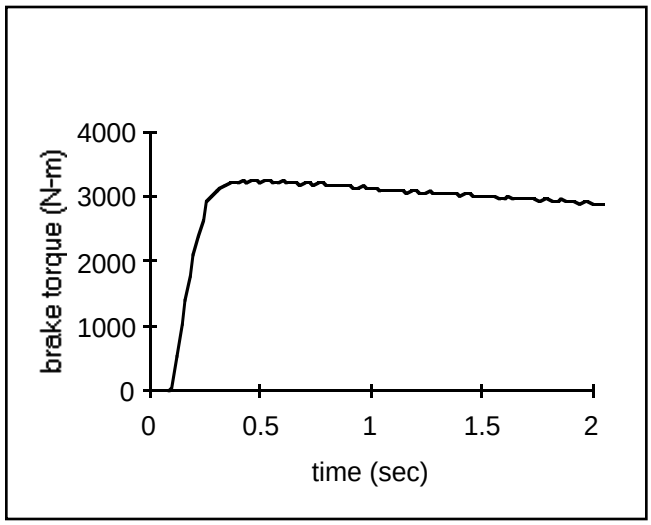

Figure 17(b): Brake torque vs time

Figure 17: Wet road, ±25% sinusoidal uncertainty, target slip = 0.20 (acceleration)

We found the traction controller described in section 3.2 to be able to maintain a target slip under different road conditions, constant uncertainty and time-varying uncertainty. The advantage of the controller is its robustness and simplicity brought about because it does not

require an estimate of $d\mu/dt$. The disadvantage is that it maintains slip at a predetermined target slip, which is not necessarily the peak slip.

If the target slip is set at the peak slip for one road condition, performance may be sacrificed at other road conditions. However, if the target slip is set low enough the system's operating point should be at or below the peak of the $\mu - \lambda$ curve for all road conditions. Acceleration will not necessarily be optimized but stability will be maintained. The loss in acceleration will most likely be insignificant compared to the robustness gained and the guarantee of stable vehicle control, which is necessary for highway automation. Because of the robustness advantages, the controller described in section 3.2 is recommended for highway automation applications.

4. EFFECT OF TRACTION CONTROL ON LONGITUDINAL PLATOON SYSTEMS

We performed simulations to investigate the effect of traction control when longitudinal platoon control is attempted on an icy road surface. The simulation study looked at the effect of traction control on longitudinal platoon control during the following three scenarios:

- Two car platoon with acceleration on an icy road
- Two car platoon with deceleration on an icy road
- Four car platoon with acceleration and deceleration on an icy road.

The simulations compare the performance of a longitudinal platoon system with and without traction control. The simulation model includes engine, vehicle, wheel and actuator dynamics (described in section 2). The vehicle parameters used in the simulations are modeled after a Lincoln Towncar and are summarized in appendix 2.

We used the target slip fuzzy logic traction controller described in section 3.2. The controller's target slip was set to 0.30, which is slightly below the peak slip of the $\mu - \lambda$ curve (fig. 1) for icy road conditions. The controller was implemented to control slip during both acceleration (anti-slip control) and deceleration (anti-lock control).

For the longitudinal platoon system we used a sliding mode longitudinal controller in D. Swaroop et. al. that attempts to maintain a constant spacing between a string of vehicles (Swaroop 1994). The controller uses the position, velocity and acceleration of the front (lead) car and the controlled vehicle's predecessor to determine the controlled vehicle's desired throttle angle and brake torque. The speed and distance of the controlled vehicle relative to its predecessor are measured by onboard sensors (for example radar or sonar). Each vehicle, including the lead vehicle may broadcast (for example by radio) its velocity, acceleration and sensor measurements to the vehicle following it. Front vehicle information is used to ensure the spacing errors are not magnified as they propagate from vehicle to vehicle. Both the traction controller and longitudinal controller output a desired or command brake torque (T_{b_tract} and T_{b_long}). We combined the traction and longitudinal controllers to regulate brake torque according to the following algorithm:

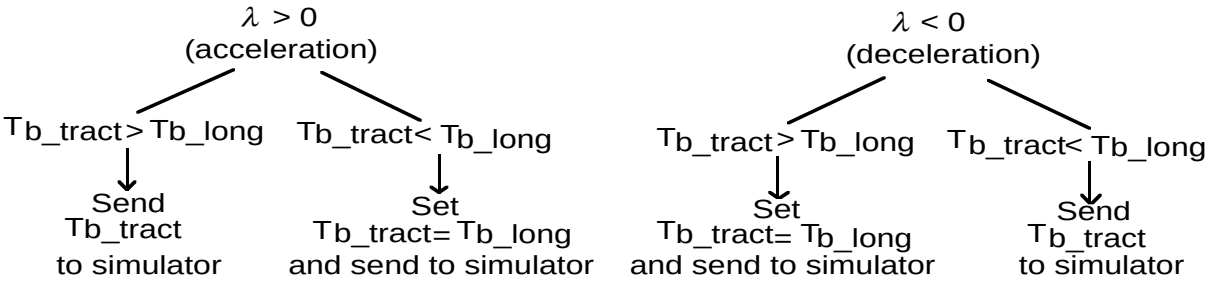

The algorithm tends to drive the slip to the target slip when fast acceleration or deceleration is required, otherwise the magnitude of slip remains below the target slip and the traction controller is ignored.

In all cases, the desired spacing (space between cars) is 2 meters. Initially, all cars start with the same velocity as the front car and a 2 meter spacing.

4.1 Simulations

Two Car Platoon with Acceleration:

The first scenario we studied was a two car platoon on an icy road with the front car accelerating from 22m/s (approx. 50mph) to 26m/s (approx. 58mph) in about five seconds (fig. 18). Figure 19 shows the results. The longitudinal controller performs significantly better with traction control.

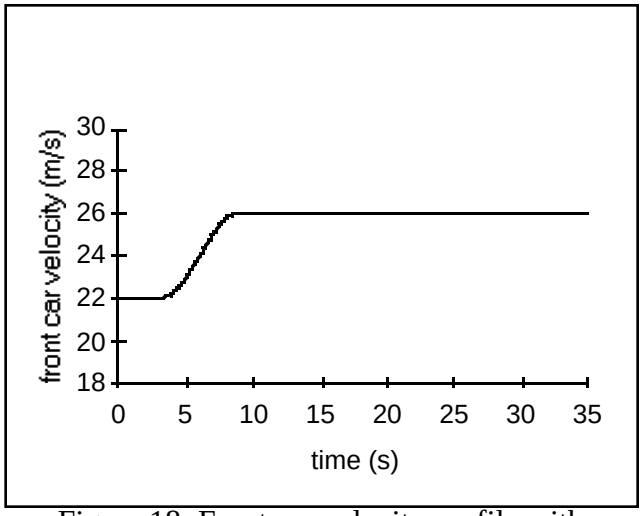

Figure 18: Front car velocity profile with acceleration

Without traction control the second car initially cannot keep up with the accelerating front car (fig. 19(a)). The car's driving wheels slip (fig. 19(c)), traction is reduced and the spacing error becomes large. Once the car does catch up, it cannot be effectively decelerated as the wheels lock-up, and the spacing error becomes negative. The result is an oscillatory spacing error with the wheel's slipping during acceleration and locking up during braking. The longitudinal control actions (brake torque, throttle angle) appear unstable (fig. 19(e,g)). With

traction control, the wheels are not allowed to slip (fig. 19(d)), traction is maximized and the second car is quickly able to catch up to the front car (fig. 19(b)). The controller outputs are stable and smooth (fig. 19(f,h)).

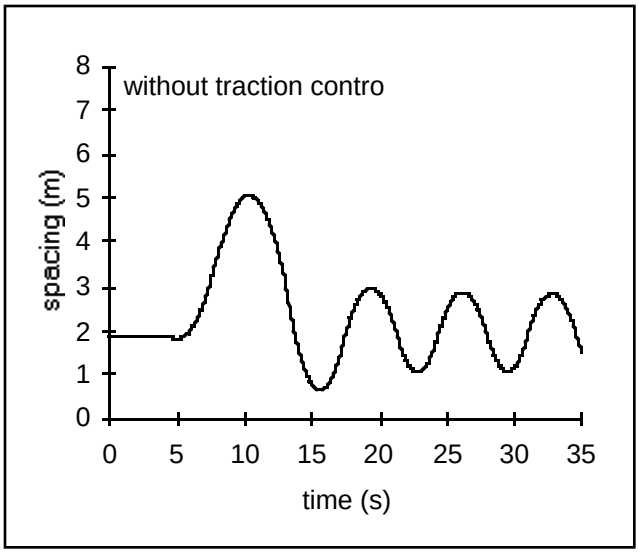

Figure 19(a): Spacing vs time (without traction control)

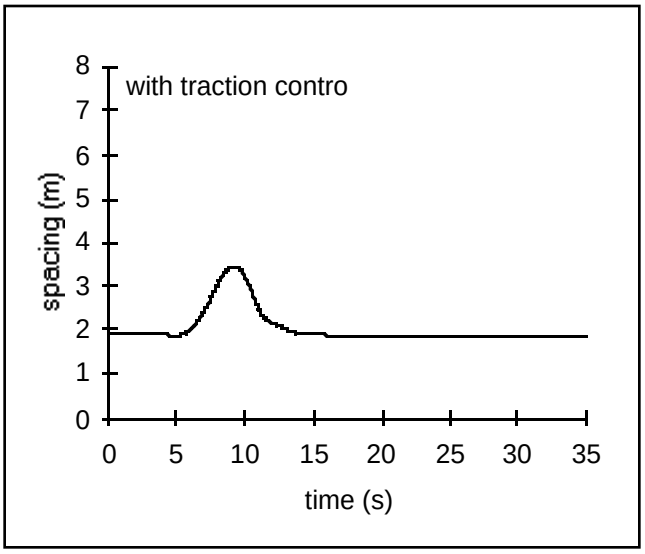

Figure 19(b): Spacing vs time (with traction control)

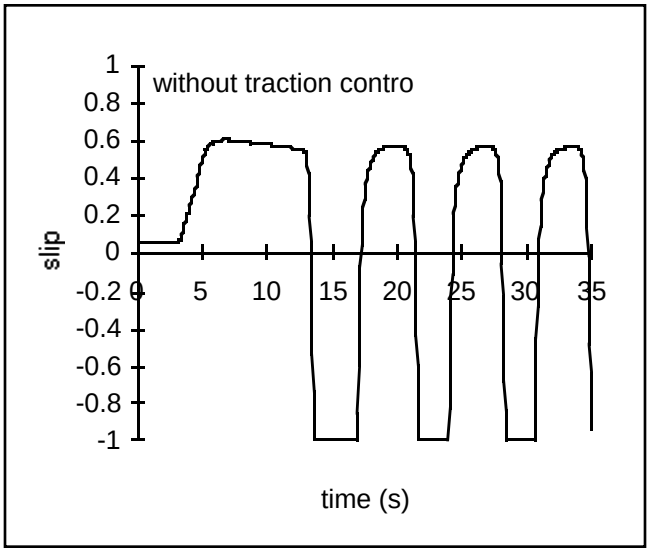

Figure 19(c): Slip vs time (without traction control)

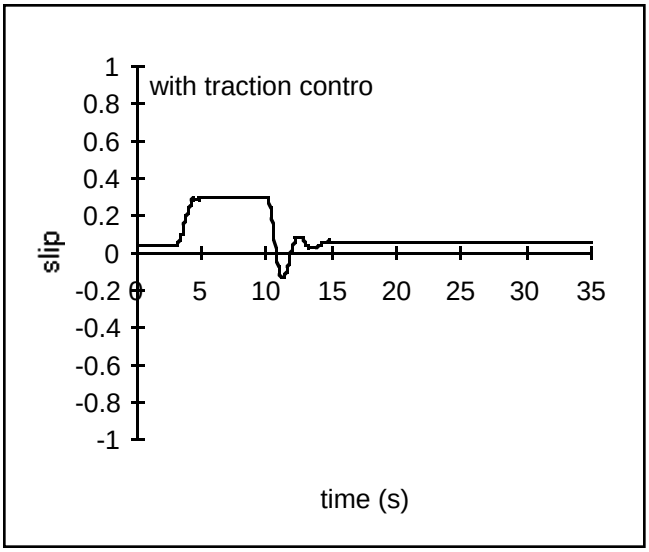

Figure 19(d): Slip vs time (with traction control)

Figure 19: Second car of two car platoon with acceleration, desired spacing = 2m, target slip = 0.30

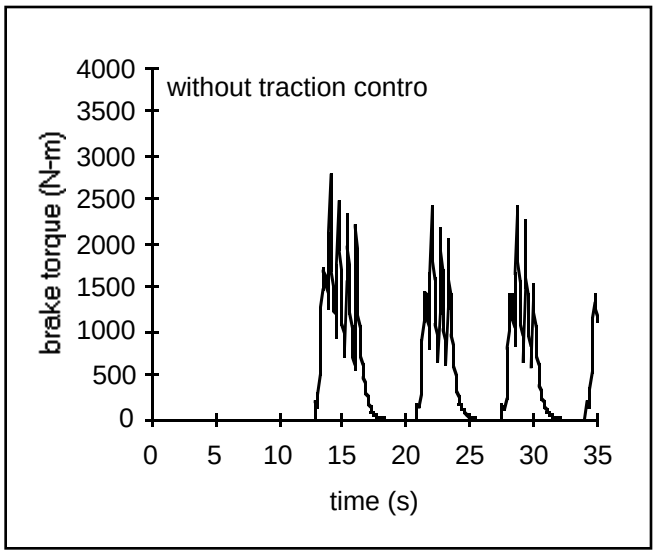

Figure 19(e): Brake torque vs time (without traction control)

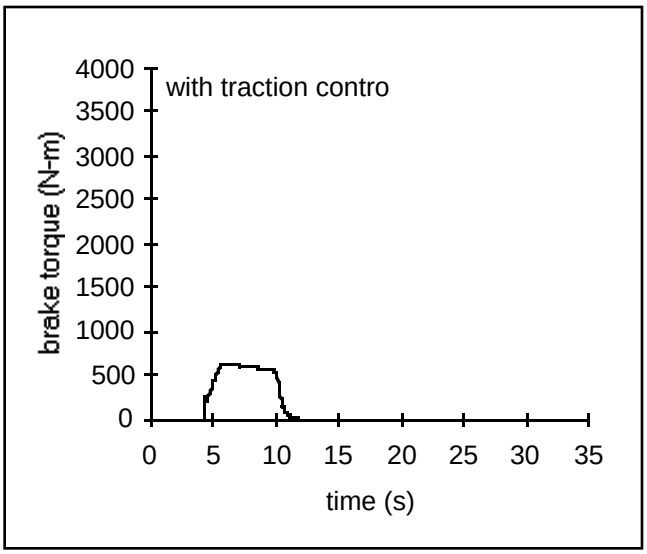

Figure 19(f): Brake torque vs time (with traction control)

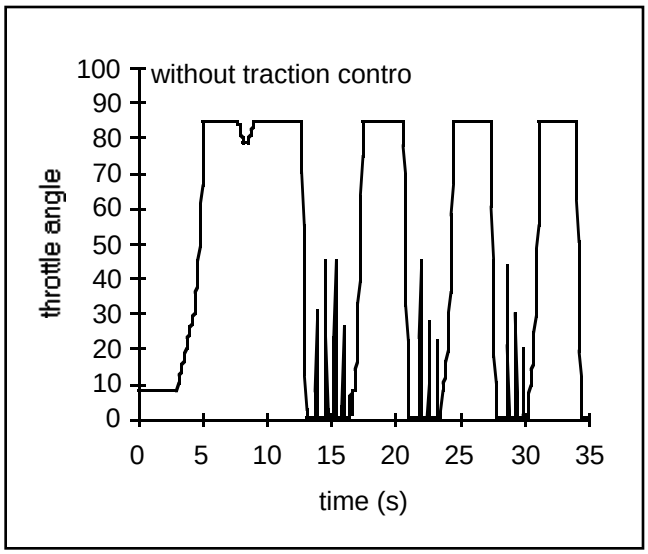

Figure 19(g): Throttle angle vs time (without traction control)

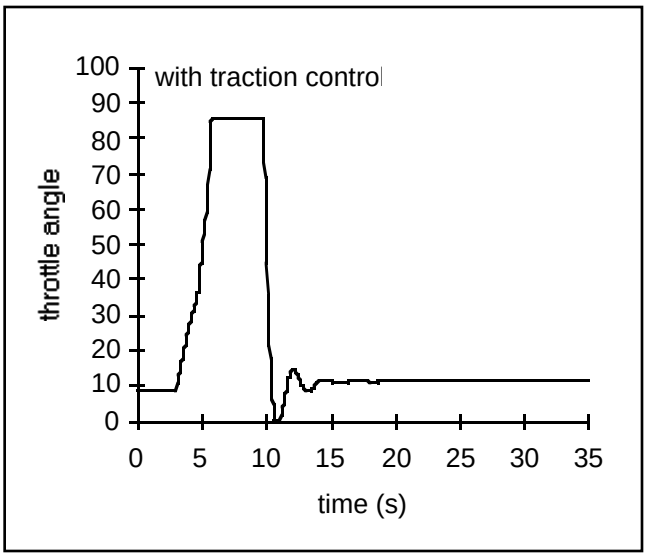

Figure 19(h): Throttle angle vs time (with traction control)

Figure 19: Second car of two car platoon with acceleration, desired spacing = 2m, target slip = 0.30

Two Car Platoon with Deceleration:

The second scenario we studied was a two car platoon on an icy road with the front car decelerating from 26m/s (approx. 58mph) to 21m/s (approx. 47mph) in about five seconds (fig. 20). Figure 21 shows the results. As in the case with acceleration, the longitudinal controller

performs significantly better with traction control. The traction controller prevents locking during braking the same way it prevents spinning during acceleration, by maintaining the magnitude of slip at or below the target slip.

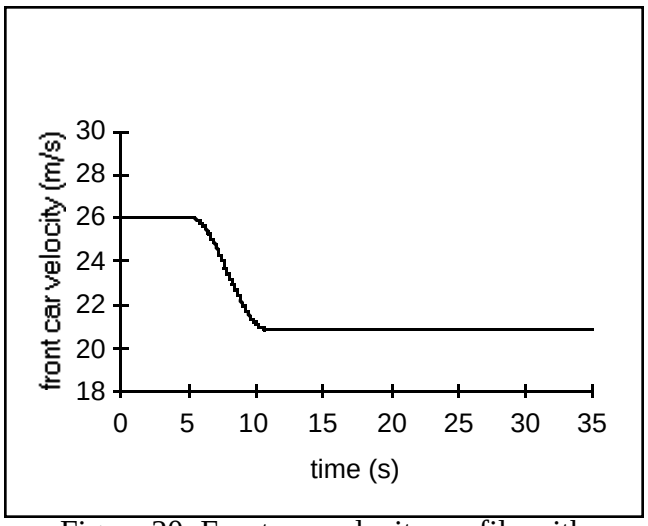

Figure 20: Front car velocity profile with deceleration

Without traction control the second car cannot be effectively decelerated as the wheel's lock-up figure (21(c)), and the spacing falls below zero indicating a collision (fig. 21(a)). As in the case with acceleration, the spacing error is oscillatory and the control actions appear unstable (figs. 21(e,g)).

With traction control, the magnitude of the wheel slip is not allowed above the target slip (fig. 21(d)), preventing the wheels from locking-up. Traction is maintained and the vehicle is quickly able to slow down to provide the desired spacing (fig. 21(b)).

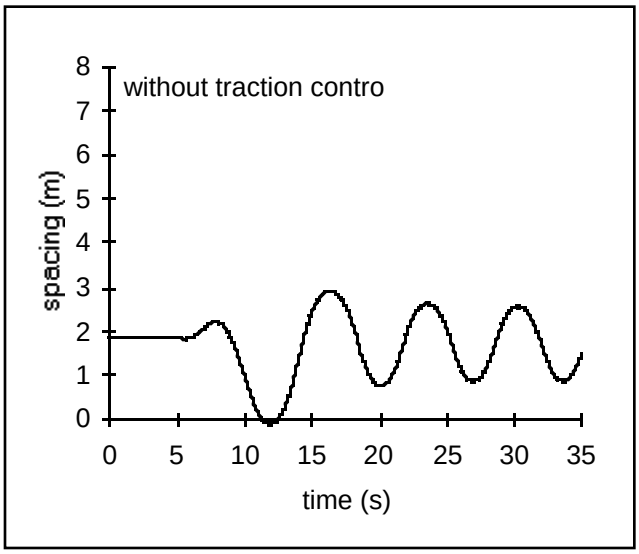

Figure 21(a): Spacing vs time (without traction control)

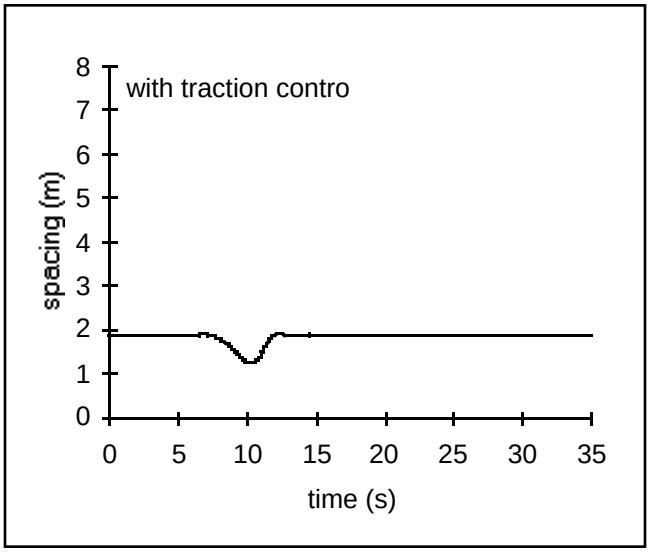

Figure 21(b): Spacing vs time (with traction control)

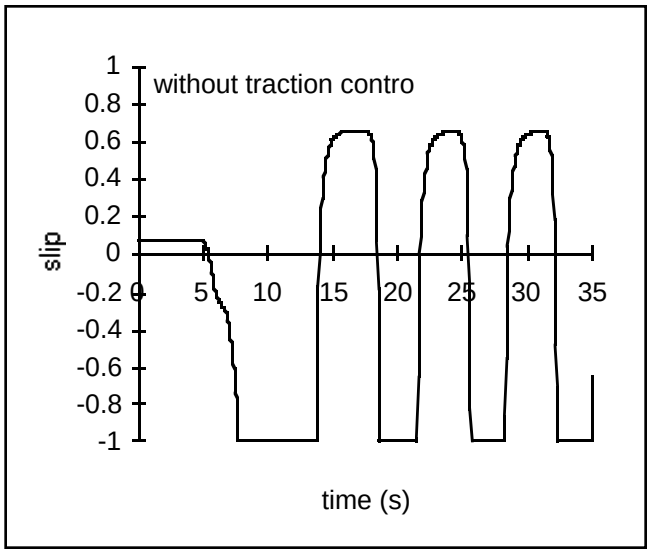

Figure 21(c): Slip vs time (without traction control)

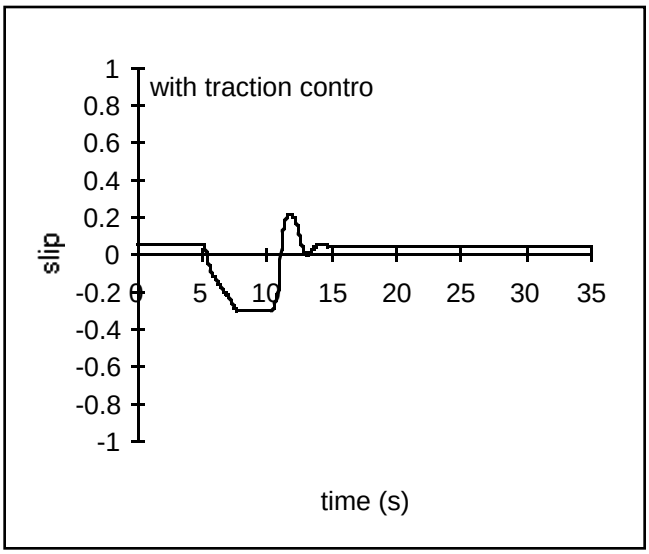

Figure 21(d): Slip vs time (with traction control)

Figure 21: Second car of two car platoon with deceleration, desired spacing = 2m, target slip = 0.30

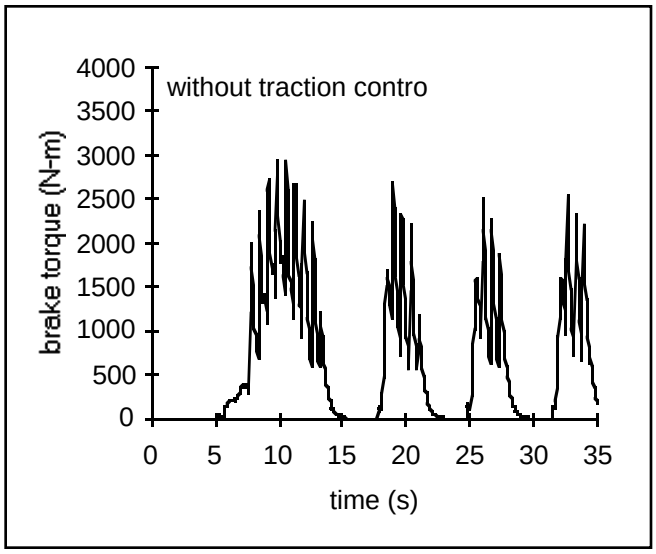

Figure 21(e): Brake torque vs time (without traction control)

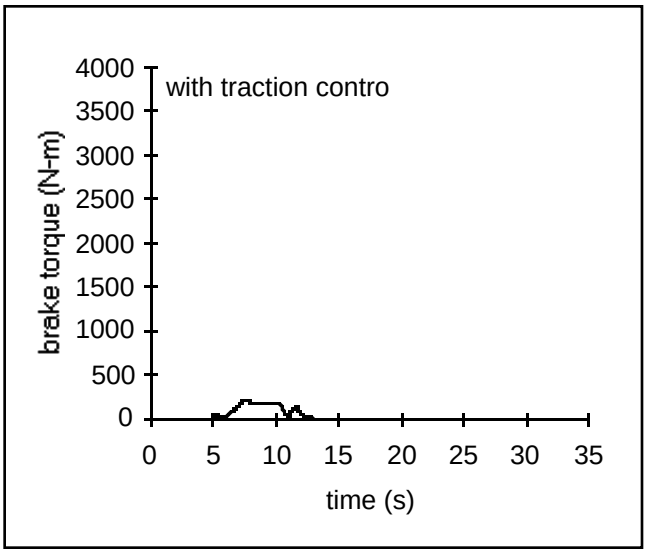

Figure 21(f): Brake torque vs time (with traction control)

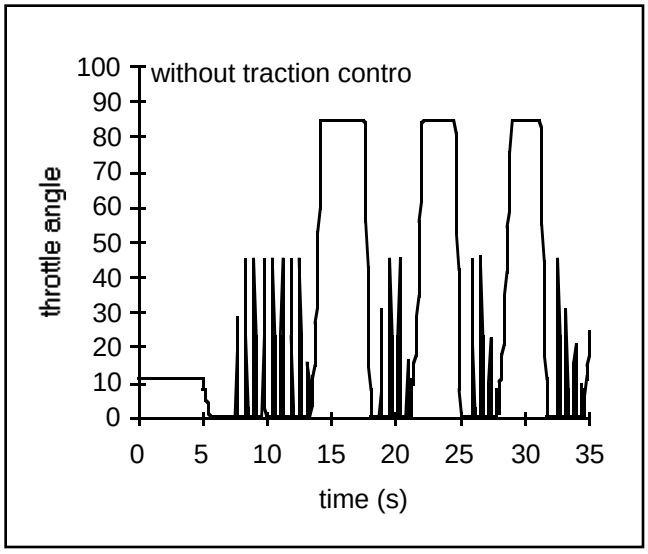

Figure 21(g): Throttle angle vs time
(without traction control)

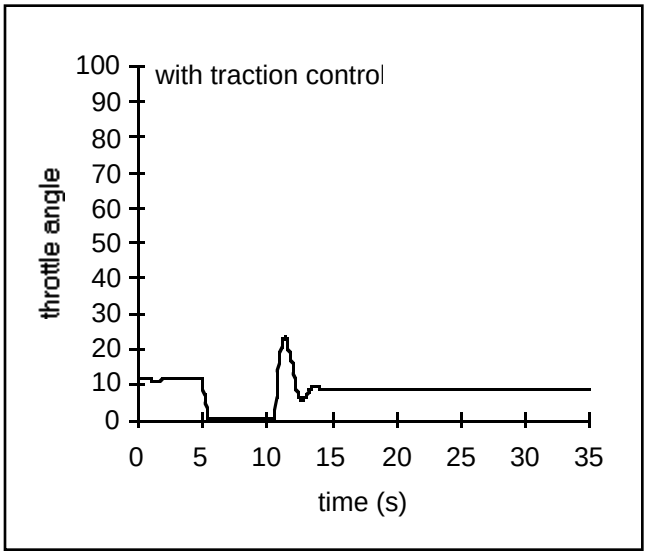

Figure 21(h): Throttle angle vs time
(with traction control)

Figure 21: Second car of two car platoon with deceleration, desired spacing = 2m, target slip = 0.30

Four Car Platoon with Acceleration and Deceleration:

The last scenario we studied was a four car platoon on an icy road with the front car accelerating from 22m/s to 26m/s and then decelerating to 22m/s (fig. 22). We combined acceleration and deceleration to provide a more severe maneuver. We added more cars to evaluate if spacing error propagates from car to car. The results are shown on figs. 23-25. The traction controller significantly improved the performance of the longitudinal platoon system.

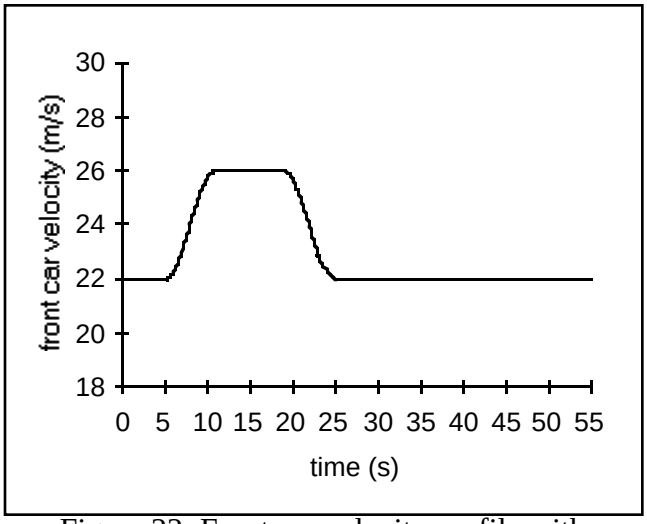

Figure 22: Front car velocity profile with acceleration and deceleration

Without traction control, the cars are unable to accelerate and decelerate effectively, causing large and oscillatory spacing errors. The spacing between cars drops below zero, indicating collisions. The wheel slip alternates between slipping and locking-up, and the control actions appear unstable.

With traction control, the wheels are not allowed to slip or lock-up and traction is maintained. The desired spacing is quickly obtained with smooth and minimal control action. The spacing error decreases from car to car along the string. As mentioned previously, the longitudinal controller utilizes front car information to prevent magnification of spacing error.

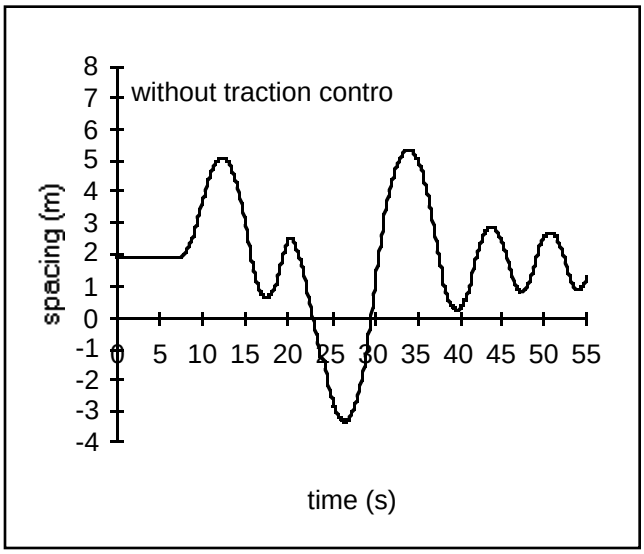

Figure 23(a): Spacing vs time (without traction control)

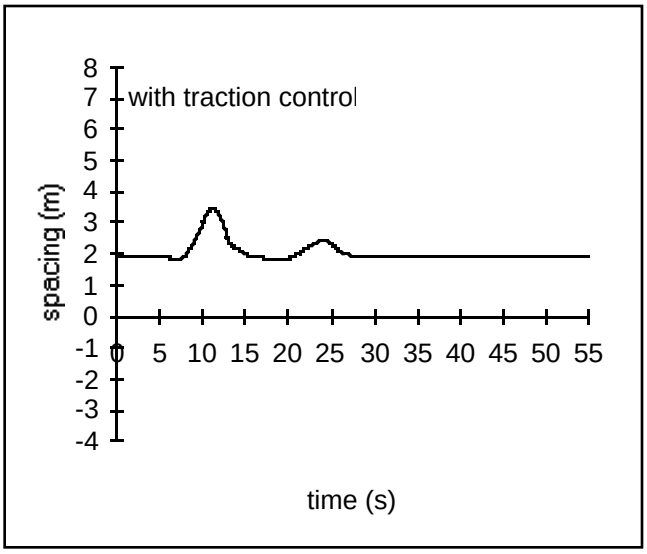

Figure 23(b): Spacing vs time (with traction control)

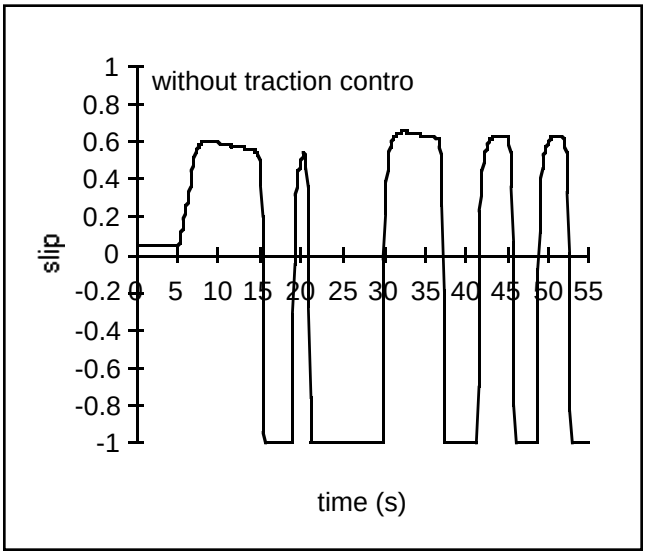

Figure 23(c): Slip vs time (without traction control)

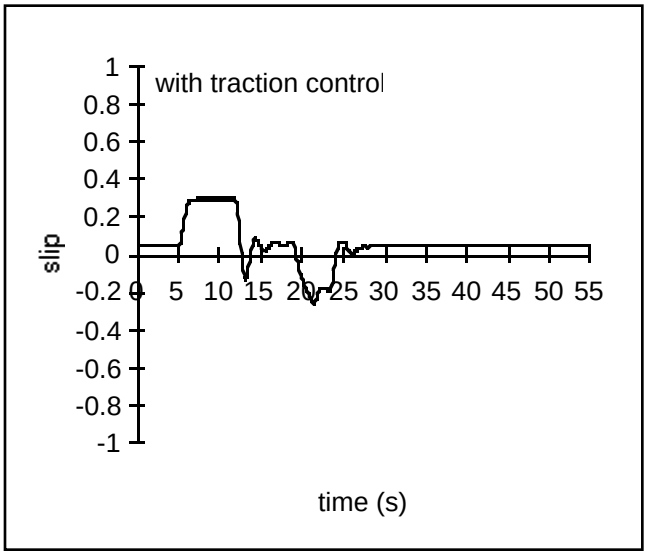

Figure 23(d): Slip vs time (with traction control)

Figure 23: Second car of four car platoon with acceleration and deceleration, desired spacing = 2m, target slip = 0.30

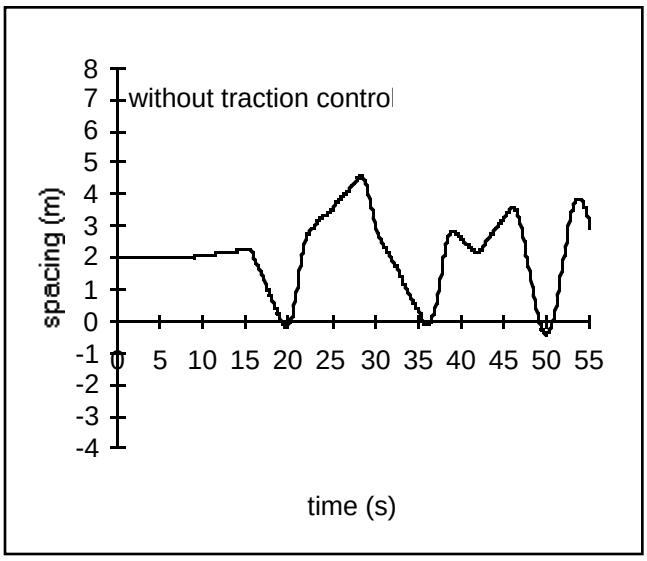

Figure 24(a): Spacing vs time (without traction control)

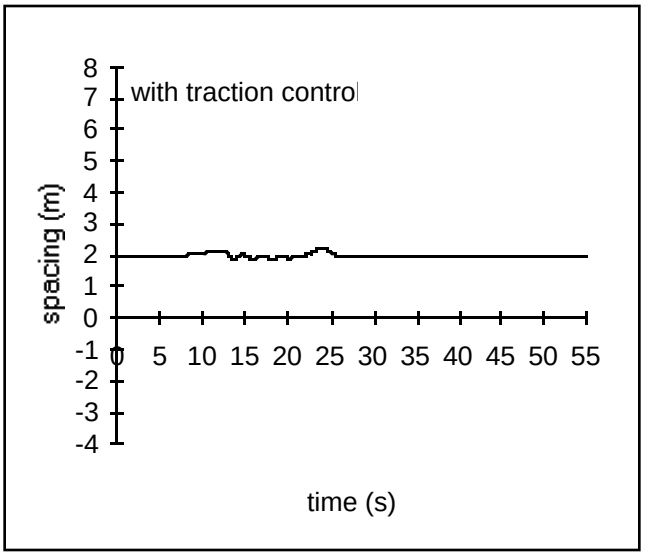

Figure 24(b): Spacing vs time (with traction control)

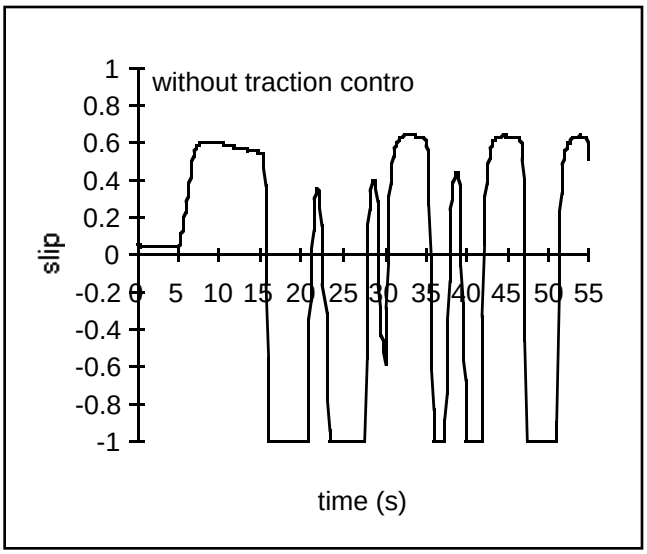

Figure 24(c): Slip vs time (without traction control)

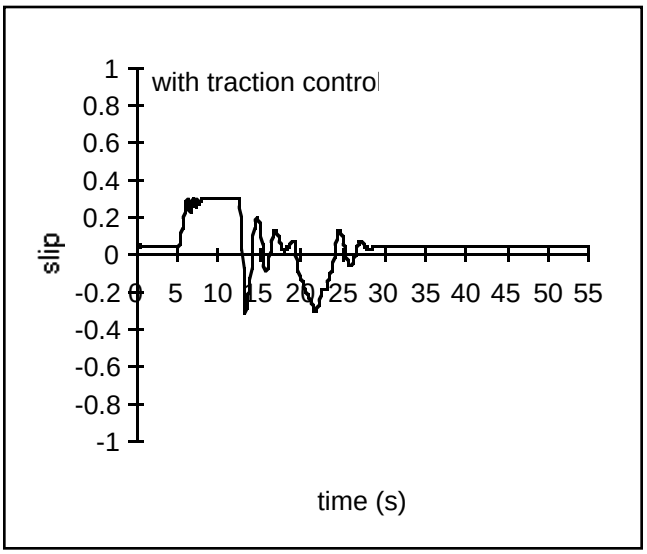

Figure 24(d): Slip vs time (with traction control)

Figure 24: Third car of four car platoon with acceleration and deceleration, desired spacing = 2m, target slip = 0.30

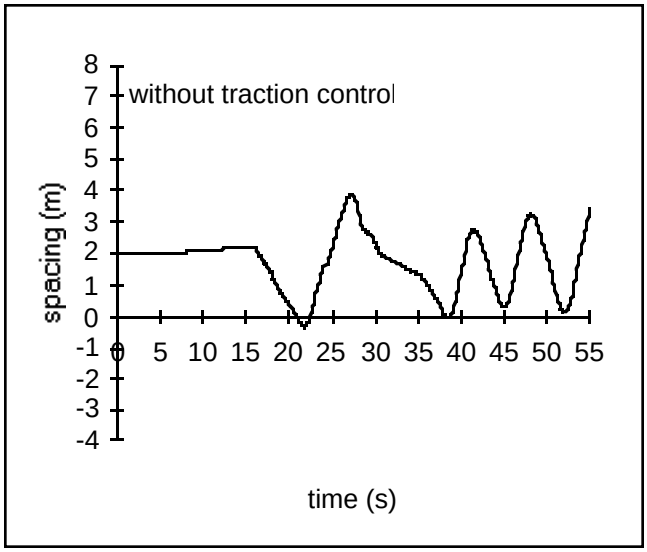

Figure 25(a): Spacing vs time (without traction control)

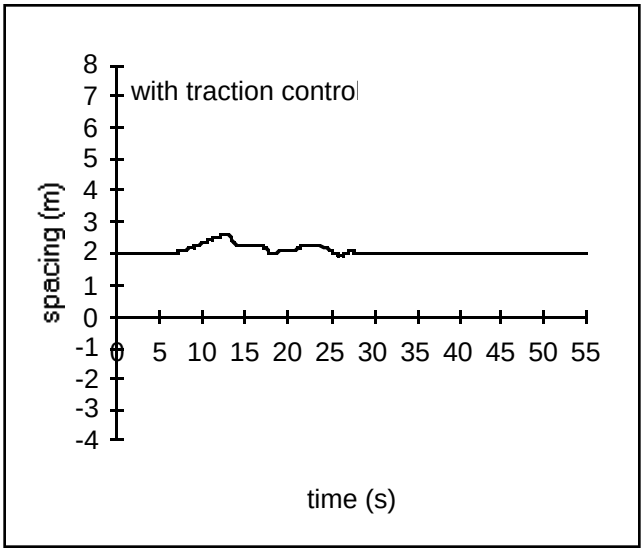

Figure 25(b): Spacing vs time (with traction control)

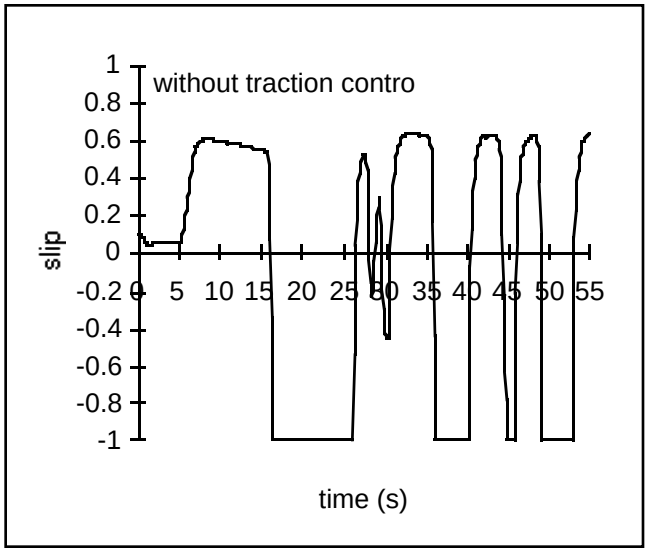

Figure 25(c): Slip vs time (without traction control)

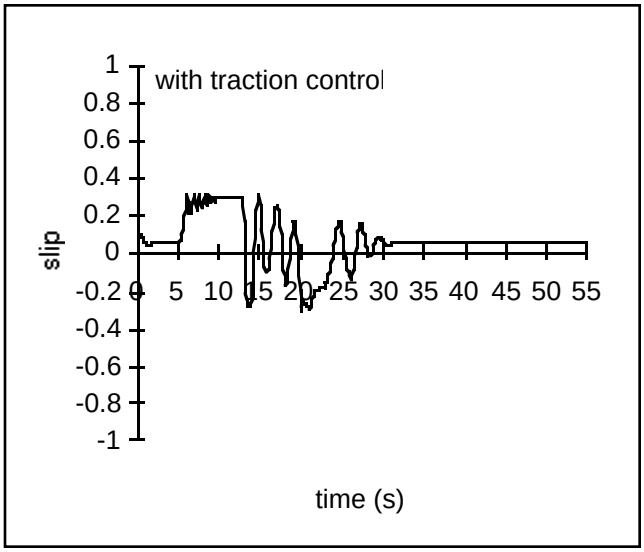

Figure 25(d): Slip vs time (with traction control)

Figure 25: Fourth car of four car platoon with acceleration and deceleration, desired spacing = 2m, target slip = 0.30

Conclusions:

The objective of this paper was to present fuzzy logic traction controllers and their effect on longitudinal platoon systems. We designed two fuzzy logic traction controllers. One controller estimates "peak slip" and regulates slip at that value. The controller is attractive because of its ability to maximize acceleration and deceleration regardless of road condition. We found through simulations that the controller's performance degrades in the presence of time-varying uncertainties. One of the controller inputs, $d\mu/dt$, is difficult to estimate from vehicle acceleration when time-varying uncertainties exist. The other fuzzy logic controller regulates slip at any desired value. Through simulations we found the controller to be robust against changing road conditions and uncertainties. The target slip is predetermined, and not necessarily the peak slip for all road conditions. However if the target slip is set low, stable acceleration and deceleration is guaranteed, regardless of road condition.

Using simulations we evaluated the effect of traction control on longitudinal platoon systems. The simulations included acceleration and deceleration maneuvers on an icy road. The results indicate traction control substantially improves longitudinal platoon performance with icy road conditions. Traction control also provides additional safety if emergency stopping or acceleration is required.

Future research, not within the scope of this report, should be performed to:

- Develop fuzzy controller that combines both brake torque and engine torque regulation.
- Enhance the fuzzy controller and longitudinal vehicle platooning simulations to include cornering maneuvers using a four-wheel (full car) model.
- Experimentally validate the fuzzy traction controllers described in sections 3.1 and 3.2.
- Experimentally demonstrate the advantages of traction control in longitudinal vehicle platoon systems.

Appendix 1: Fuzzy Logic Controllers

Fuzzy logic controllers are based on fuzzy set theory (Zadeh 1956). Fuzzy sets allow imprecise and qualitative information to be expressed in a qualitative way (Tong 1977). Both fuzzy and crisp sets, A, can be expressed in terms of a membership function, μ_A. The difference between fuzzy and crisp sets is that the membership function of a fuzzy set can take all values between 0 and 1, while the membership function of a crisp set can take only two values, 0 or 1. With fuzzy sets, the qualitativeness of a measure can be reflected by a gradual membership transition, allowing different degrees of membership (fig. 26(a)). The crisp set has a definite transition from membership to non-membership, and allows only full membership or non-membership (fig. 26(b)). Fuzzy sets allow qualitative information to be represented mathematically and handled in a rigorous manner (Tong 1977).

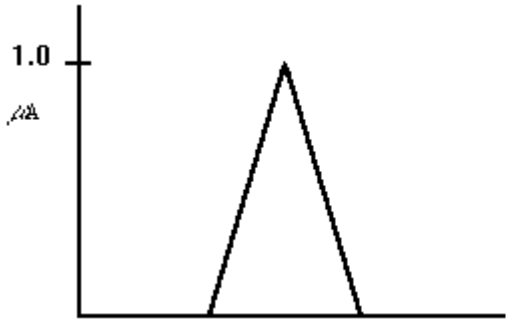

Figure 26(a): Triangular membership function for fuzzy set, A

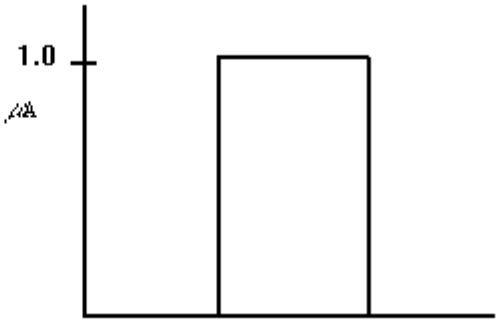

Figure 26(b): Square membership function for crisp set, A

Figure 26: Typical membership functions for fuzzy and crisp sets

The fuzzy logic controller is based on linguistic rules, such as " if input A is large and input B is small, then output C is small". Controller inputs, which are a crisp set of numbers usually measured by sensors, are converted to fuzzy variables and sent to the fuzzy logic controller. The controller produces a fuzzy output which is then defuzzified and the crisp output is sent to the plant. Figure 27 depicts the fuzzy logic control system.

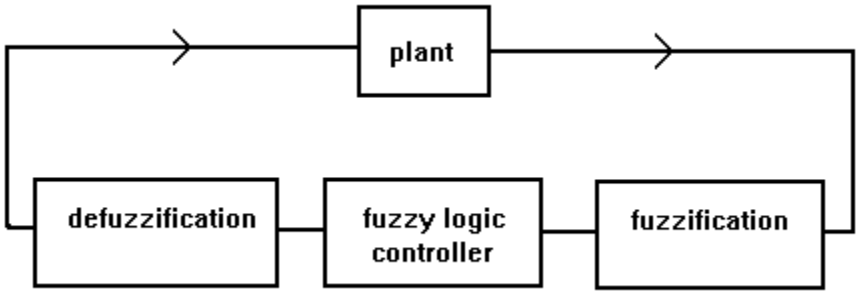

Figure 27: Fuzzy Logic Control System

Fuzzification:

During the fuzzification process, controller inputs are matched against the membership functions of the linguistic categories, resulting in fuzzy variables. The fuzzy variables may acquire membership ranging from 0 to 1. When designing a fuzzy controller, one must determine the type of membership functions and the number of linguistic categories. Typical membership functions are monatomic, triangular, trapezoidal or bell shaped (Kandel 1994). The number of categories determines the level of granularity for describing each fuzzy variable. Figure 28 shows triangular membership functions for a set of five linguistic categories; positive big, positive small, zero, negative small and negative big. In this case, the controller input, x, has 0.7 membership in the zero category ($\mu_{zo}(x) = 0.7$), 0.3 membership in the positive small category ($\mu_{ps}(x) = 0.3$), and non-membership in the rest.

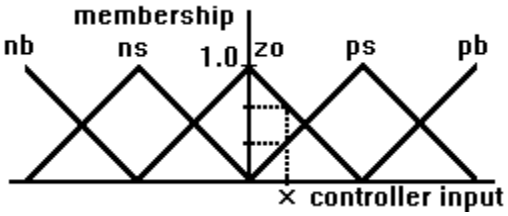

Figure 28: Triangular membership function with five grades

Fuzzy Control:

The fuzzy controller consists of linguistic "if then" rules. The rules are typically generated from an expert's experience and knowledge, from system models and from human operator models (Kandel 1994). Since a controller input may have partial membership in multiple linguistic categories, several rules may fire at once. A process of conflict resolution is used to determine what control action should be taken as a result of the firing of several rules (Kandel 1994). A typical conflict resolution process is based on Larson's product rule (Lee 1990). The following example illustrates the process. Assume we have two controller inputs, x and y, one controller output, z, and two fuzzy rules:

If x is big and y is big, then z is big. (rule 1)
If x is small and y is small, then z is small. (rule 2)

Each rule's firing strength (α) is calculated as the minimum membership value of all variables in the rule. For example, the strength of rules 1 and 2 are determined from:

$\alpha_1 = \min(\mu_{big}(x), \mu_{big}(y))$ (for rule 1)
$\alpha_2 = \min(\mu_{small}(x), \mu_{small}(y))$ (for rule 2)

The recommended control action for each control rule is represented as a membership function. The rule's fuzzified output ($\mu_1(z)$ and $\mu_2(z)$) are defined as the minimum of the rule's firing strength and the rule's output membership function.

$\mu_1(z) = \min(\alpha_1, \mu_{big}(z))$ (for rule 1)
$\mu_2(z) = \min(\alpha_2, \mu_{small}(z))$ (for rule 2)

Both rules recommend a fuzzy control action. The conflict resolution process provides a combined fuzzy control action ($\mu(z)$) in the form of a membership function and is defined as the maximum of $\mu_1(z)$ and $\mu_2(z)$ over the possible range of the output, z:

$$\mu(z) = \max(\mu_1(z), \mu_2(z))$$

Figure 29 shows graphically how the fuzzy control actions for both rules ($\mu_1(z)$ and $\mu_2(z)$) are obtained. Figure 30 shows the combined fuzzy control action ($\mu(z)$).

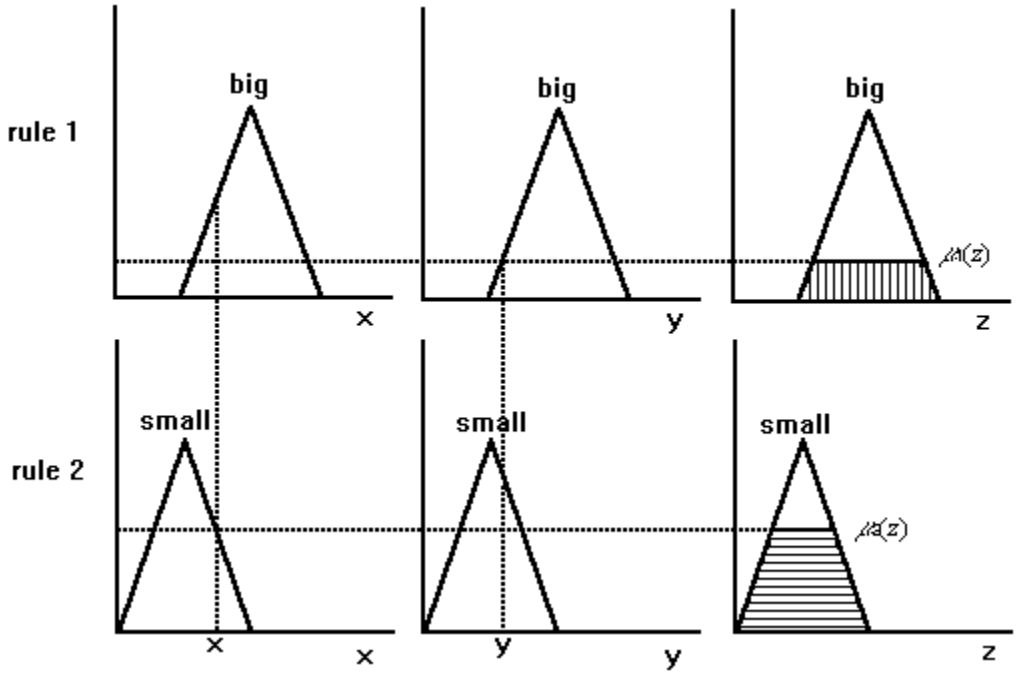

Figure 29: Fuzzy control outputs ($\mu_1(z)$ and $\mu_2(z)$) for rules 1 and 2

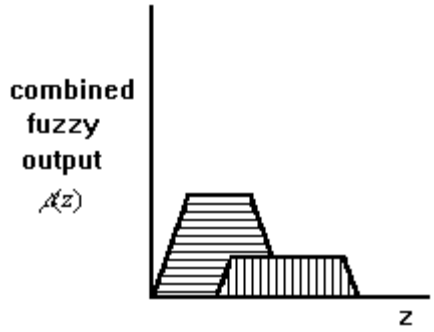

Figure 30: Combined fuzzy control output ($\mu(z)$)

Defuzzification:

The next step is to defuzzify the fuzzy control output to produce a crisp (non-fuzzy) output, Z, which can be sent to the plant. Some defuzzification strategies include the center of area method, the mean of maximum method and Tsukamoto's method. We will concentrate on the center of area method, which is a popular defuzzification strategy (Kandel 1994). We assume the output (z) has been descretized with "q" quantization levels. The method calculates the center of area of the combined fuzzy control output ($\mu(z)$):

$$Z = \frac{\sum_{j=1}^{q} z_j \cdot \mu(z_j)}{\sum_{j=1}^{q} \mu(z_j)}$$

Appendix 2: Simulation Parameters

Vehicle Parameters

The vehicle parameters used in the simulations were modeled after a Lincoln Towncar. The air mass flow rate ($\dot{m}_{ai}$) and engine torque (T_e) were provided by the engine manufacturer as a look up table.

J = wheel inertia = $2.656\ (kg\text{-}m^2)$

R_w = wheel radius = $0.3307\ (m)$

Nv = normal load on tire = $6000\ (N)$ (estimated from vehicle mass)

M_v = car mass = $2148\ (kg)$

N_w = number of driving / braking wheels = 2

C = wind drag coefficient = 0.53384

final drive speed reduction ratio = 0.305
first gear seed reduction ratio = 0.4167
second gear speed reduction ratio = 0.6817
third gear speed reduction ratio = 1.0
fourth gear speed reduction ratio = 1.4993
brake torque time constant = 0.4 (s) (reduced from 0.8 to accommodate traction control)
throttle actuator time constant = 0.011 (s)
maximum throttle angle = 85.0 (deg)
minimum throttle angle = 0.0 (deg)
maximum throttle rate = 450.0 (deg/s)

References:

Duengen, R. 1989. The Application of the COP888 to a 2-wheel ABS System. *Electronic Engineering*, Vol. 61, No. 748.

Harned, J. L. et al.1969. Measurement of Tire Brake Force Characteristics as Related to Wheel Slip Control System Design. *SAE Trans.*, Vol. 78, No. 690214.

Kachroo, P.. and M. Tomizuka. 1994. Vehicle Traction Control and Its Application. California PATH Research Paper, UCB-ITS-PRR-94-08.

Kandel, A., and G. Langoholz. 1994. *Fuzzy Control Systems*, CRC Press, Boca Raton.

Kiyotaka, I., K. Fujita, Y. Inoue and S. Masutomi. 1990. The Lexus Traction Control (TRAC) System. *SAE Transactions*, Vol. 99, Sect. 6, pp. 319-326.

Kraft, H. J., and H. Leffler. 1990. The Integrated Brake and Stability Control System of the New BMW 850i. *SAE Transactions*, Vol. 99, Sect. 6, pp. 263-270.

Layne, J., K. Passino and S. Yurkovich. 1993. Fuzzy Learning Control for Anti-skid Braking Systems. *IEEE Trans. on Control Systems Technology*, Vol. 1, No. 2.

Lee, C. C. 1990. Fuzzy Logic in Control Systems: Fuzzy Logic Controller, part I and II. *IEEE Trans. on Syst., Man. and Cybern.*, Vol. SMC-20, No. 2, pp. 404-435.

Leiber, H.,and A. Czinczel. 1983. Four Years of Experiences with 4-Wheel Anti-skid Brake (ABS). SAE 830481.

Miyasaki, N., M. Fukumoto, Y. Sogo and H. Tsukinoki. 1990. Anitilock Brake System (M-ABS) Based on the Friction Coefficient Between the Wheel and the Road Surface. *SAE Special Publications*, No. 815.

Miyashita, I., T. Sasaki and Y. Ohmori. 1993. A Fuzzy Anti-slip Control for Electric Motor Coach. Proceedings of IEEE International Workshop on Neural-Fuzzy Control, Muroran, Japan.

Rittmannsberger, I. N. 1988. Anti-lock Braking Systems and Traction Control. *IEEE*.

Schurr H., and A. Dittner. 1984. A New Anti-skid Brake System for Disc and Drum Brakes. *Braking: Recent Developments*, SAE 840486.

Sigi, A., and H. Demel. 1990. ASR-Traction Control, State of the Art and Some Prospectives. *SAE Transactions*, Vol. 99, Sect. 6, pp. 263-270.

Swaroop, D., J. K. Hedrick, C. C. Chien and P. Ioannou. 1994. A Comparison of Spacing and Headway Control Laws for Automatically Controlled Vehicles. Vehicle System Dynamics Journal, 23, pp25-53.

Tan, H. S. 1988, Adaptive and Robust Controls with Application to Vehicle Traction Control. Ph.D. Dissertation, University of California, Berkeley.

Tan, H. S., and M. Tomizuka. 1989. Discrete-Time Controller Design for Robust Vehicle Traction. *American Control Conference*.

Tomizuka, M.,and J. K. Hedrick. 1993. Automated Vehicle Control for IVHS Systems. Presented at IFAC Conference.

Tong, R. M. 1977. A Control Engineering Review of Fuzzy Systems. *Automatica*, Vol. 13, pp. 559-569.

Wang, L. W. 1992. Stable Adaptive Fuzzy Control of Nonlinear Systems. *Proceedings of the 31st Conf. on Decision and Control.*

Zadeh, L. A. 1965. Fuzzy Sets. *Information Control*, Vol. 8, No. 3.